

Comparative Direct Analysis of Type Ia Supernova Spectra. III. Premaximum

David Branch¹, M. A. Troxel¹, David J. Jeffery¹, Kazuhito Hatano², Miriam Musco³, Jerod Parrent¹, E. Baron¹, Leeann Chau Dang^{1,4}, D. Casebeer¹, Nicholas Hall¹, & Wesley Ketchum¹

ABSTRACT

A comparative study of spectra of 21 Type Ia supernovae (SNe Ia) obtained about one week before maximum light, and 8 spectra obtained 11 or more days before maximum, is presented. To a large extent the premaximum spectra exhibit the defining characteristics of the four groups defined in Paper II (core-normal, broad-line, cool, and shallow-silicon). Comparisons with SYNOW synthetic spectra show that all strong features and most weak ones can be accounted for in a plausible way. The issues of detached high-velocity features, the possible ubiquity of carbon clumps, the maximum detectable ejecta velocities, and the possibility of blueshifted emission-line peaks are discussed.

Subject headings: supernovae: general

1. INTRODUCTION

This is the third in a series of papers on a comparative direct analysis of the optical spectra of Type Ia supernovae (SNe Ia). Paper I (Branch et al. 2005) was concerned with a time series of spectra, from 12 days before to 115 days after the time of maximum light, of the well-observed, spectroscopically normal, Type Ia SN 1994D. Paper II (Branch et al. 2006) concentrated on near-maximum-light spectra of 24 SNe Ia. In this paper we focus on pre-maximum-light spectra, which form in the outermost layers of the ejected matter and provide clues to the nature of the explosions that cannot be obtained from later

¹Homer L. Dodge Department of Physics and Astronomy, University of Oklahoma, Norman, OK 73019; e-mail: branch@nhn.ou.edu

²Division of Network Business, PionetSoft Corporation, Shibuya-ku, Tokyo 151-0072, Japan

³Department of Astronomy, Indiana University, Bloomington, IN 47405

⁴Department of Astronomy, Whitman College, Walla Walla, WA 99362

spectra that form deeper in the ejecta. Our emphasis is on line identifications, which are needed in the quest to develop good hydrodynamical explosion models for SNe Ia. When detailed spectrum calculations are carried out for explosion models (e.g., Baron et al. 2006; Howell et al. 2001), discrepancies between synthetic and observed spectra invariably appear. Knowing the identities of the observed features provides clues to how the explosion models should be modified in order to achieve better agreement with observation.

In Paper II we divided the maximum–light spectra into four groups: *core–normal*; *broad–line*; *cool*; and *shallow–silicon* (denoted CN, BL, CL, and SS, respectively, in the figures and tables of this paper). The group assignments were made on the basis of measurements of the (pseudo) equivalent widths of absorption features near 5750 Å and 6100 Å, as well as on the appearance (depth, width, and shape) of the 6100 Å absorption, which is produced by the Si II λ 6355 transition. Although we framed the presentation and discussion in terms of the four groups, in the end we concluded that for the most part the spectra appeared to have a continuous distribution of properties, rather than consisting of discrete subtypes. Therefore, exactly how the group boundaries were drawn was not important.

Figure 1, a plot of the equivalent width $W(5750)$ of the absorption feature near 5750 Å against the equivalent width $W(6100)$ of the absorption feature near 6100 Å in maximum–light spectra, is an update of the corresponding figure in Paper II, with the following additional events: the core–normal SN 2003cg (Elias–Rosa et al. 2006), SN 2003du (Gerardy et al. 2004), and SN 2004S (Krisciunas et al. 2006); the broad–line SN 1983G (McCall et al. 1984) and SN 2002er (Kotak et al. 2006); and the shallow–silicon SN 1999aa (Garavini et al. 2004), SN 1999ac (Garavini et al. 2005), SN 2000E (Valentini et al. 2003), SN 2005cg (Quimby et al. 2006), and SN 2003fg [the proposed super–Chandrasekhar SN Ia, also known as SNLS-03D3bb; Howell et al. (2006); Jeffery, Branch, & Baron (2007a); but see also Hillebrandt, Sim, & Röpke (2007)]. SN 1999ac is a borderline case: in Figure 1 it falls between two core–normals but on the basis of the shape, depth, and width of the 6100 Å absorption, we include it with the shallow–silicons.

To a large extent the premaximum spectra turn out to exhibit the defining characteristics of the four maximum–light groups of Paper II, so we use the same terminology in this paper (with all group assignments based on maximum–light, not premaximum, spectra). Again, we are not suggesting that SNe Ia actually consist of discrete subtypes; instead, we are thinking in terms of three inhomogeneous groups radiating outward (in Figure 1) from the highly homogeneous core normals.

In Figure 1, three lines of constant $W(5750)/W(6100)$ ratio are shown. This ratio is similar to although not the same as the well known $R(Si II)$ ratio (Nugent et al. 1995), which is based on the depths of the same two absorption features. Considerable diversity

at a given $W(5750)/W(6100)$ ratio is evident, especially at the low value of 0.05, e.g., the SN 2005hk, SN 1999ee, and SN 2002bf have similar $W(5750)/W(6100)$ ratios but otherwise their spectra are very different.

In this paper, as in Papers I and II, we confine our attention to optical spectra, from the Ca II H&K feature in the blue (~ 3700 Å) to the Ca II infrared triplet (Ca II IR3) in the red (~ 9000 Å). All spectra have been corrected for the redshifts of the parent galaxies. The original spectra have a range of slopes, owing to intrinsic differences, differences in the amount of reddening by interstellar dust, and observational error. Because we are interested only in the spectral features, and not in the underlying continuum slopes, all spectra in this paper, both observed and synthetic, have been flattened according to the local normalization technique of Jeffery et al. (2007b). The flattening facilitates comparison of the spectral features. Mild smoothing also has been applied to some of the spectra.

We examined all of the SN Ia premaximum spectra available to us and selected two samples: a “one-week premax” sample, consisting of one spectrum each of 21 SNe Ia observed between day -5 and day -9 with respect to the time of maximum brightness in the B band, and an “early” sample, consisting of one spectrum each of eight SNe Ia observed on or earlier than day -11 . (All SNe of the early sample are also in the one-week premax sample.) The SNe Ia and the epochs of the selected spectra are listed in Table 1.

Continuing our attempt to provide an internally consistent quantification of SN Ia spectra, we have used the SYNOW code to fit all spectra of Table 1. Descriptions of SYNOW and its use can be found in Branch et al. (2003) and Paper I¹. Compared to other supernova synthetic-spectrum codes, SYNOW is simple, but when working in an empirical spirit from the data, as opposed to evaluating an explosion model, SYNOW offers the advantage that the user has direct control over line optical depths as function of radial coordinate, while other codes input composition and density structures and then compute the temperature structure and the line optical depths. Thus SYNOW is the most useful code for making line identifications (pending eventual confirmation by means of detailed calculations for explosion models whose spectra and light curves match the observations). For the present work, we adopt precepts for fitting spectra that are much like those of Paper II, e.g., the default excitation temperature is 7000 K for the cool SN 1986G and SN 1999by and 10,000 K for all others.

¹For consistency with Papers I and II, in this paper we do not use SYNOW version 2.0, described and used by Parrent et al. (2007).

2. CORE-NORMALS

Figure 2 shows the spectra of the seven core-normals of the one-week premax sample. The spectrum of SN 2001el differs from the others; as shown by Mattila et al. (2005), it resembles the day -14 spectrum of SN 1990N, so it will be discussed below, with the early sample. The other spectra show considerable homogeneity, although the diversity is somewhat greater than in the maximum-light core-normal sample. The 6100 \AA absorption is deeper in SN 1998bu and SN 2003cg than in the others, and the broad absorption near 4300 \AA is weaker in SN 1994D and SN 1998aq than in the others. SN 2003du has strong HV² Ca II absorptions near 3700 \AA and 8000 \AA (although not nearly as strong as in the exceptional SN 2001el). SN 1990N also has a strong absorption near 3700 \AA . Diversity in HV Ca II was present also in maximum-light spectra of core-normals.

The SYNOW fitting parameters for core normals of the one-week premax sample are in Table 2. An example fit, to the day -7 spectrum of SN 2003du, is shown in Figure 3. The fit is good and most of the line identifications seem clear. The most obvious discrepancy, the failure of the synthetic spectrum to match the observed absorption near 3980 \AA , is primarily caused by Si II $\lambda 4130$, so we can not remove this discrepancy without doing harm to the fit elsewhere.

The synthetic absorption produced by Si III $\lambda 4560$ is a bit too blue to match the observed absorption at 4400 \AA (which is present in most observed spectra of this paper). A better fit could be achieved by using C III $\lambda 4649$ instead of Si III. But in a synthetic spectrum that contains only Si III lines the $\lambda 4560$ absorption does occur at the right place to account for the 4400 \AA absorption, and Si III $\lambda 5743$ also accounts for a weak observed absorption near 5560 \AA . In most premaximum spectra there is little or no evidence for C II features, so it would be surprising to see ubiquitous evidence for the high-excitation (29.6 eV) C III line. Therefore, even though neither Si III feature fits well in the full synthetic spectrum (the $\lambda 5743$ absorption does not even appear as a distinct feature), we assume that these two Si III lines usually are responsible for the corresponding observed features.

The synthetic absorption produced by Si II $\lambda 5972$ does not account well for the observed absorption at 5750 \AA . This and the other two discrepancies mentioned above are generic to our fits. The fit could be improved by invoking Fe III lines with a higher excitation potential, at or approaching $15,000 \text{ K}$, so that lines near 6000 \AA contribute to the 5750 \AA absorption [see Branch et al. (2003) on SN 1998aq]. But the problem with the 5750 \AA absorption

²As in Papers I and II, PV refers to features that form at or near the photospheric velocity and HV refers to high-velocity detached features.

occurs in some spectra in which we see no evidence for the stronger Fe III lines in the blue, so we refrain from using high-excitation Fe III to resolve this discrepancy. Another way to improve the fit, in some cases, would be to use a higher Si II optical depth and impose a maximum velocity on Si II (see §3 and §4).

In our fits to the core normals of the one-week premax sample, the relative weakness of the absorption near 4300 Å in SN 1994D and SN 1998aq is accounted for by using lower Mg II and Fe III optical depths (see Table 2). In the same two SNe we have used C II lines, to allow $\lambda 6580$ to improve the fit near the peak of the Si II $\lambda 6355$ feature.

Figure 4 shows the spectra of the three core-normals (and the two broad-lines, to be discussed in §3) of the early sample. The diversity among the core-normals of the early sample is much greater than in the one-week premax sample, e.g., the three 6100 Å absorptions have distinctly different shapes, and in SN 1994D the absorption trough from 4600 to 5000 Å is deeper than in SN 1990N and SN 2003du. The early spectrum of SN 1994D is an example of group crossover: the spectrum is more like that of the broad-line SN 2002bo than like the other core-normals. (On the other hand, the spectrum of the broad-line SN 2002er could pass for core-normal.)

The SYNOW fitting parameters for the three core-normals (and the two broad-lines) of the early sample are in Table 3. The deeper 4600 Å to 5000 Å absorption trough in SN 1994D is accounted for primarily by using stronger HV Fe II.

How to fit the various shapes of the 6100 Å absorption is an interesting issue. For SN 1994D we fit it in the conventional way, with a simple PV Si II component (a fit is shown in Paper I). For SN 2003du, the feature appears to consist of two marginally resolved components (Stanishev et al. 2007), so we use both PV and HV Si II. The fit is shown in Figure 5. (We did not need to use HV Si II for the one-week premax spectrum of SN 2003du.)

The unusual, nearly flat-bottomed 6100 Å absorption of the early spectrum of SN 1990N has been discussed by several authors (Jeffery et al. 1992; Fisher et al. 1997; Mazzali 2001). Mattila et al. (2005) showed that the one-week premax spectrum of SN 2001el resembled the early spectrum of SN 1990N (see their Figure 1). As can be seen by comparing our Figures 2 and 4, the HV absorption of the Ca II infrared triplet is much deeper in SN 2001el (requiring a covering factor approaching unity), but otherwise the two spectra, including the 6100 Å absorption, are quite similar. Mattila et al. attributed the flat-bottomed shape of the 6100 Å absorption to line formation in a shell that is geometrically thin compared to the size of the photosphere, but this explanation is not viable. Line formation in a thin shell that is not detached from the photosphere does produce a (shallow) flat-bottomed absorption [see Figure 8 of Jeffery & Branch (1990)], but the blue edge of the absorption is blueshifted only

by an amount that corresponds to the photospheric velocity, which is not the case in the spectra of SN 1990N and SN 2001el. We can nicely fit the flat-bottomed absorptions with a single Si II component, using a high value of v_e and imposing a maximum velocity. However, since the blue edge of the absorption corresponds to a high velocity comparable to that at which the HV Ca II and HV Fe II are forming ($\sim 20,000 \text{ km s}^{-1}$), it seems more reasonable to assume that the feature is an unresolved blend of PV and HV components, and fit the absorption accordingly (see Table 2 for SN 2001el and Table 3 for SN 1990N). Support for this interpretation is provided by a previously unpublished spectrum of SN 1990N obtained at day -12 in bad weather by S. Benetti and M. Turatto (Figure 6). The absorption feature resembles the marginally-resolved two-component absorptions of SN 2003du (Figure 5) and SN 2005cg (Figure 13). [see also Garavini et al. 2007 on 05cf]

3. BROAD-LINES

Figure 7 shows the spectrum of the core-normal SN 2003du (for comparison) and the spectra of the four broad-lines of the one-week premax sample. In maximum-light spectra (Paper II) broad-lines have the same spectral features and line identifications as core-normals, but the equivalent width of the 6100 \AA absorption is larger and the features are generally broader. The four broad-lines of Figure 7 also have these characteristics, although as in Paper II, the borderline case SN 1992A differs from core-normal mainly in the depth and equivalent width of the 6100 \AA absorption. SN 2002er is much like SN 1992A except for a weaker absorption near 7450 \AA . As at maximum light, SN 1984A is the most extreme broad-line in the sample.

The SYNOW fitting parameters for broad-lines of the one-week premax sample are listed in Table 4. As at maximum light (Paper II), the one-week premaximum spectra of the broad-lines can be fitted with the same ions as used for the core-normals, but with higher values of v_e and/or τ .³ Figure 8 shows our fit to the day -7 spectrum of the extreme broad-line SN 1984A. For Si II a high value of $v_e = 4000 \text{ km s}^{-1}$ is used and a maximum velocity of $27,000 \text{ km s}^{-1}$ is imposed.

The spectra of the two broad-lines of the early sample are shown in Figure 4, and fitting parameters are in Table 3. Fe III is not used for the early spectra of the broad-lines, but its features could be hidden by the strong HV Fe II lines. Figure 9 shows our fit to the day -14

³When inspecting fitting parameters one should keep in mind the partial degeneracy of v_e and τ . For example, for SN 2002bo the synthetic absorption produced by Si II $\lambda 6355$ with $\tau = 7$ and $v_e = 2000 \text{ km s}^{-1}$ is roughly similar to the corresponding absorption in SN 1992A with $\tau = 45$ and $v_e = 1000 \text{ km s}^{-1}$.

spectrum of SN 2002bo. In an attempt to account for the 5750 Å absorption with Si II λ 5972 we have used a large optical depth of 30 for Si II and imposed a maximum velocity of 25,000 km s⁻¹. A maximum velocity of 22,000 km s⁻¹ has been imposed on S II.

4. COOLS

Figure 10 shows the spectrum of the core-normal SN 2003du and the spectra of the three cools of the one-week premax sample. For reasons given in Paper II, the borderline SN 1989B was included in the cool group even though it did not show the blue trough from about 4000 Å to 4300 Å that is characteristic of the other cools. Here again SN 1989B has a higher $W(6100)$ value than core-normals and resembles SN 1986G at wavelengths longer than about 4400 Å, while lacking the blue trough. SN 1989B remains a borderline case.

The SYNOW fitting parameters for cools of the one-week premax sample are listed in Table 5. At maximum light (Paper II) our strategy when attempting to simultaneously account for the 5750 Å and 6100 Å absorptions was to use a high optical depth and impose a maximum velocity on Si II (as we have done in this paper for some of the broad-lines; see §3). Figure 11 shows our fit to the day -5 spectrum of SN 1999by, where we have used the same strategy with only partial success; in the synthetic spectrum, the 5750 Å absorption is too weak even though the 6100 Å is too strong. We regard the line identifications in Figure 11 to be definite, except for Sc II, which helps in one place but cannot be considered definite.

There are no cools in the early sample. Only a small number of cools have been observed at all, and because they have short rise times and are dim relative to other SNe Ia, no spectra have been obtained at times as early as day -11.

5. SHALLOW-SILICONS

Figure 12 shows the spectra of the core-normal SN 2003du and the seven shallow-silicons of the one-week premax sample. These were classified as shallow-silicon on the basis of their maximum-light spectra but they also have shallow-silicon at one-week premax. (SN 1999ac is borderline in this respect but it is more like the shallow-silicons than the core normals in other respects, such as in having weak S II absorptions.) There is plenty of diversity, however, extending to the extreme cases of SN 1991T and its near twin SN 1997br which at a glance do not necessarily have Si II at all (although we do include it in our fits), and to SN 2005hk. SN 2005hk is in our one-week premax sample of shallow-silicons (with fitting

parameters in Table 6 the same as used in Chornock et al. 2006), and SN 2002cx was in our maximum-light sample of shallow-silicons. But as discussed in Paper II and elsewhere (Li et al. 2003; Branch et al. 2004b; Jha et al. 2006; Chornock et al. 2006; Stanishev et al. 2007; Phillips et al. 2007), in spite of certain spectroscopic similarities to SN 1991T-like, the SN 2002cx-like appear to be physically distinct from other SNe Ia.

The fitting parameters for the shallow-silicons of the one-week premax sample are in Table 6. The shape of the 6100 Å absorption in SN 2005cg is especially interesting, because it appears to consist of marginally resolved PV and HV components of Si II. Our fit is shown in Figure 13. Note that in Figure 12 the 6100 Å absorption of SN 1999ee bears some resemblance to that of SN 2005cg. As with the one-week premax spectrum of SN 2001el and the early spectrum of SN 1990N, the 6100 Å absorption of SN 1999ee can be fit with a single broad PV component or an unresolved combination of a PV and an HV feature. For the same reasoning as in the discussion of SN 1990N and SN 2001el and the results of Garavini et al. (2007) and Stanishev et al. (2007), we use the two components.

Figure 14 shows the spectra of the core-normal SN 2003du and the three shallow-silicons of the early sample. Again SN 1999aa and SN 1991T do have shallow silicon, and again SN 1999ac is borderline. Figure 15 shows our fit to the day –12 spectrum of SN 1999aa. Like Garavini et al. (2004), we have resorted to C III, but the identification is not definite. When fitting the HV Ca II infrared triplet absorption, the HV Ca II H&K absorption comes out too deep; this happens in some of our other fits, although less than here. We believe the absorption feature near 5500 Å to be Si III λ 5743, but as usual it does not appear as a distinct feature in the synthetic spectrum.

6. DISCUSSION

The previous sections have been organized in terms of the four groups of Paper II, with all group assignments based on the appearance of near-maximum-light spectra. To a large extent the one-week premax spectra of this paper retain the defining characteristics of the four groups, i.e., group assignments based on one-week premax spectra would be much the same. To a lesser extent, the same is true of the early spectra of this paper, e.g., almost all shallow-silicons are distinct from core-normals (Figure 14). But there is some crossover between groups in the early sample, e.g., Figure 4 shows that the early spectra of the core-normal SN 1994D and the broad-line SN 2002er are not very different. In any case, as in Paper II we see little or no evidence that SNe Ia actually break up into distinct groups, except for the SN 2002cx-like (and possibly the cools, but see Pastorello et al. 2007 on SN 2004eo for evidence of a connection between core normals and cools).

The SYNOW fits to the premaximum spectra of this paper generally are of the same quality as the fits to the maximum–light spectra of Paper II. All strong features and most weak ones can be accounted for in a plausible way. Most line identifications seem clear, although as discussed in previous sections there are some ambiguities, and some of the weak features remain unidentified. For the most part our line identifications in premaximum spectra are consistent with those suggested previously on the basis of SYNOW (or SYNOW–like) synthetic spectra, as well as synthetic spectra calculated with the Mazzali–Lucy Monte Carlo code. Such studies have been carried out for SN 1990N (Jeffery et al. 1992; Mazzali et al. 1993; Mazzali 2001), SN 1991T (Ruiz–Lapiente et al. 1992; Jeffery et al. 1992; Mazzali, Danziger, & Turatto 1995; Fisher et al. 1999), SN 1997br (Hatano et al. 2002), SN 1998aq (Branch et al. 2003), SN 1999aa (Garavini et al. 2004), SN 1999ac (Garavini et al. 2005), SN 1999ee (Mazzali et al. 2005a), SN 2002bo (Benetti et al. 2004; Stehle et al. 2005), SN 2003cg (Elias-Rosa et al. 2006), and SN 2005hk (Chornock et al. 2006).

One of the notable differences from line identifications in some of the previous papers is that neither in this paper nor in Paper II do we use PV Fe II or Co II (except in SN 2005hk). In Paper I on SN 1994D we first used weak PV Fe II at day +4, and at later epochs it became much stronger. This appears to be consistent with the argument of Kasen & Woosley (2007) that the development of extensive line blocking by PV Fe II (and Co II) lines soon after maximum light is the key to understanding the SN Ia width–luminosity relation (Phillips et al. 1999). We will return to this issue in Paper IV, on post–maximum SN Ia spectra.

We do use PV Fe III for the one–week premax sample, except in the cools. It is commonly said, correctly, that SN 1991T–likes are characterized by conspicuous Fe III features. It is not true, though, that the Fe III features are particularly strong in SN 1991T–likes. At one–week premax we use Fe III optical depths for the shallow–silicons that are comparable to or lower than for the core–normals and the broad–lines. The same was true at maximum light (although we failed to mention it in Paper II). At maximum and one–week premax, Fe III features are conspicuous in shallow–silicons only because there is less competition from other features.

It is interesting to consider some of the implications of the fitting parameters, especially the line optical depths, in the context of the local–thermodynamic–equilibrium (LTE) calculations of Hatano et al. (1999a). For example, Figure 5 of Hatano et al. shows that in LTE near 7500 K the Si II optical depth can exceed unity in a composition in which hydrogen and helium have burned to carbon and oxygen while the mass fraction of other elements, including silicon, is only solar. This suggests that the presence of Si II in the spectrum does not necessarily require synthesized silicon. However, for this composition the optical depth of Fe II is predicted to be greater than that of Si II, which according to us is not

the case in premaximum or near–maximum spectra. Figure 6 of Hatano et al. shows that for a carbon–burned composition, which does include synthesized silicon, the Si II optical depth exceeds that of Fe II by a large factor. Therefore, since we do not use PV Fe II in premaximum and maximum spectra, we expect that wherever PV Si II is detected, it is produced by synthesized, rather than primordial, silicon. Another interesting example is that for the core–normals of the one–week premax sample, the Si II optical depths range from four to eight (and for the core–normals of the maximum–light sample it ranged from six to 13). Figure 6 of Hatano et al., for the carbon–burned composition, shows that a temperature difference of only 800 K is sufficient to change the Si II optical depth by a factor of two. This temperature sensitivity makes the high degree of homogeneity among the core–normals all the more remarkable.

The HV features are intriguing. Following the discovery of HV Ca II and HV Fe II in SN 1994D (Hatano et al. 1999b), HV Ca II has been recognized by many authors: see Li et al. (2001), Thomas et al. (2004), and Branch et al. (2004a) on SN 2000cx; Wang et al. (2003), Kasen et al. (2003), and Mattila et al. (2005) on SN 2001el; Mazzali et al. (2005a) on SN 1999ee; Gerardy et al. (2004) and Stanishev et al. (2007) on SN 2003du; Quimby et al. (2006) on SN 2005cg; and Garavini et al. (2007) on SN 2005cf. In premaximum spectra of SNe Ia, HV Ca II is ubiquitous (Mazzali 2005b; and this paper), and in Paper II and we regularly invoked HV Ca II even at maximum light. The identification of HV Fe II, which usually appears at modest strength in a crowded spectral region, is perhaps not definite, but we have invoked it regularly both in this paper and in Paper II at maximum light. One thing that is clear, from flux spectra (Thomas et al. 2004; Tanaka et al. 2006) and especially from polarization measurements (Wang et al. 2003; Kasen et al. 2003), is that in at least some cases the HV Ca II features form in asymmetrical structures. The *origin* of the HV features is unclear. One possibility is that for one reason or another they form naturally in the ejecta (Hatano et al. 1999b). An alternative, favored by Gerardy et al. (2004) and Quimby et al. (2006), is that they form in a shell of restricted velocity interval and elevated density that is produced by interaction between the ejecta and circumstellar matter (an accretion disk, a filled Roche lobe, or a common envelope). Our identification of HV Fe II, if correct, may hint that the features can form naturally in the ejecta, because more often than not we detected HV Fe II at a lower velocity than HV Ca II. In the spectra of the early sample, it is unlikely that the HV Fe II features are produced by iron resulting from decay the decay of ^{56}Ni and ^{56}Co , because lines of HV Ni II and HV Co II also would be expected (see Figure 9 of Hatano et al. 1999a), but it is possible that the HV Fe II features are produced by iron that has been freshly synthesized along with ^{56}Ni . Another hint that the HV features may arise naturally in the ejecta is that in some cases we see HV Si II at about the same velocity as HV Ca II and HV Fe II. In the circumstellar interaction scenario, the blue wing of the

Si II absorption is predicted to be truncated rather than extended (Gerardy et al. 2004; Quimby et al. 2006). In any case, it is interesting that that HV features, of Ca II, Fe II, and Si II typically are detached not far from 20,000 km s⁻¹. The density and/or composition structure of most SNe Ia seems to have something special around 20,000 km s⁻¹, probably including a density increase (Mazzali et al. 2005a; Mazzali 2005b).

The day -14 spectrum of the broad-line SN 2002bo (Figure 8 and Table 3) raises an issue about the definition of HV and PV features. We did not use HV Ca II or HV Si II, and what we called HV Fe II was only mildly detached, at 22,000 km s⁻¹, from the photosphere at 20,000 km s⁻¹. Thus the absence of HV Ca II or HV Si II is a matter of definition: Ca II and Si II are forming at 20,000 km s⁻¹, as in other SNe Ia, but they are not referred to as HV simply because of the high velocity at the photosphere.

The issue of carbon also is interesting for constraining explosion models. As discussed in §2, a C III line could be used to improve our fits for core-normals but we suspect that it would be spurious. We have used C III to improve the fits for several shallow-silicons but in no case is the identification convincing. Marion et al (2006) have established that C I lines are not detected [except in cools: Howell et al. (2001)], but their conclusion that carbon is much less abundant than oxygen depends strongly on their assumption of LTE at 5000 K. A temperature of 5000 K seems too low to account for the strengths of other lines (e.g., Fe III) and at higher temperatures the upper limit on the carbon-to-oxygen ratio would be much lower (see Figure 5 of Hatano et al. 1999a).

Lines of C II offer the best prospects for detecting the presence of carbon. Evidence has been presented for the strongest optical C II line, λ 6580, in SN 1998aq (Branch et al. 2003); SN 1990N (Jeffery et al. 1992; Mazzali 2001); SN 1999ac (Garavini et al. 2005); and SN 1994D and SN 1996X (Branch et al. 2003 and Paper I). Thomas et al. (2007) presented the most convincing evidence, in SN 2006D. A λ 6580 absorption was clearly present at day -7 and day -5, and it weakened as maximum light was approached. In this paper we have invoked C II in these events and only one other: the early spectrum of SN 2003du, but in this case C II λ 6580 is being used mainly just to beat down the Si II λ 6355 emission peak and the identification is not convincing. Thus, even at premaximum, C II is elusive, or, as Thomas et al. put it, sporadic, perhaps due to its tendency to appear in clumps. If the clumps are few in number and none happen to be in front of the photosphere, no absorption features will be seen. Even if a clump is in front of the photosphere, if it has sufficiently high line-of-sight velocity (about 15,000 km s⁻¹ or more) the λ 6580 absorption may be blueshifted into the Si II absorption and not be detectable. Therefore, although C II is seen in only a fraction of premaximum SN Ia spectra, the ubiquitous presence of carbon clumps in the outer layers of SNe Ia is not excluded. Unburned carbon at the observed velocities is

not characteristic of published delayed–detonation models.

Another issue to be addressed on the basis of premaximum spectra is that of the maximum detectable ejection velocities. From Figures 2, 4, 7, 10, 12, and 14 we can see that Ca II absorption is generally detectable up to about 25,000 km s⁻¹ and sometimes up to about 30,000 km s⁻¹. The highest maximum velocity that has been imposed on Ca II is 34,000 km s⁻¹ for SN 2001el. Detectable optical depth in Ca II can easily be produced with a solar mass fraction of Ca II, so the maximum velocities of synthesized Ca II may be lower. From the same figures we can see that Si II absorption is generally detectable up to 15,000 km s⁻¹ and sometimes above 20,000 km s⁻¹. The highest maximum velocity that has been imposed on Si II is 27,000 km s⁻¹ for the one–week premax spectrum of SN 1984A. We have argued above that this absorption is produced by synthesized silicon. This is consistent with the 11,900 km s⁻¹ that Mazzali, Benetti, & Hillebrandt (2007) adopted for a lower limit to the top of the silicon–rich layer, but the silicon–rich layer seems to generally extend to much higher velocities. Such high silicon velocities are not characteristic of pure deflagration models. The presence of carbon at intermediate velocities and silicon at high velocities could be consistent with the pulsating reverse detonation models of Bravo & Garcia–Senz (2006).

Another velocity–related issue is the possibility that some of the P–Cygni emission components are blueshifted, as they sometimes are in SNe II (Chugai 1988; Dessart & Hiller 2005). From measurements of the wavelengths of flux maxima Blondin et al. (2006) inferred emission–line blueshifts of up to 8000 km s⁻¹ in premaximum SN Ia spectra. The assumptions on which SYNOW is based (sharp photosphere and resonant scattering) do not allow blueshifts of unblended emission–line peaks, yet our fits do not in general have a problem reproducing the wavelengths of the observed flux maxima. In SYNOW synthetic spectra the flux maxima are affected by line blending; sometimes they are a bit too red, consistent with an emission–line blueshift, but equally often they are a bit too blue. In SNe Ia, line blending is a serious problem for establishing that emission–line peaks are blueshifted.

The premaximum spectra of SNe Ia exhibit a rich diversity, which even within each of our four groups probably is multidimensional. The outer layers of SN Ia ejecta differ in composition, density, and temperature structure, and they have asymmetries - probably both global shape asymmetries as well as composition clumping. Understanding the observational diversity in terms of the physical differences is a challenging task that will require more observations and modeling. Flux spectra have much to tell us, but in view of the asymmetries, polarization spectra are a high priority.

We are grateful to Stefano Benetti and Massimo Turatto for providing the previously unpublished spectrum of SN 1990N, and to all observers who have provided their published spectra. This work has been supported by NSF grants AST-0204771 and AST-0506028, and

NASA LTSA grant NNG04GD36G.

REFERENCES

- Anupama, G. C, Sahu, D. K., & Jose, J. 2005, *A&A*, 429, 667
- Baron, E., Bongard, S., Branch, D., & Hauschildt, P. H. 2006, *ApJ*, 645, 480
- Benetti, S., et al. 2004, *MNRAS*, 348, 261
- Blondin, S., et al. 2006, *ApJ*, 131, 1648
- Branch, D., Baron, E., Hall, N., Melakayil, M., & Parrent, J. 2005, *PASP*, 117, 545 (Paper I)
- Branch, D., et al. 2003, *AJ*, 126, 1489
- Branch, D., et al. 2004a, *ApJ*, 606, 413
- Branch, D., et al. 2004b, *PASP*, 116, 903
- Branch, D., et al. 2006, *PASP*, 118, 560 (Paper II)
- Bravo, E., & Garcia-Senz, D. 2006, *ApJ*, 642, L157
- Chornock, D., et al. 2006, *PASP*, 118, 722
- Chugai, N. N. 1988, *Sov. Astron. Lett.*, 14(5), 334
- Cristiani, S., et al. 1992, *A&A*, 259, 63
- Dessart, L., & Hillier, D. J. 2005, *A&A*, 437, 667
- Elias-Rosa, N., et al. 2006, *MNRAS*, 369, 1880
- Fisher, A., Branch, D., Hatano, K., & Baron, E. 1999, *MNRAS*, 304, 67
- Fisher, A., Branch, D., Nugent, P., & Baron, E. 1997, *ApJ*, 481, L89
- Garavini, G., et al. 2004, *AJ*, 128, 387
- Garavini, G., et al. 2005, *AJ*, 130, 2278
- Garavini, G., et al. 2007, *A&A*, in press
- Garnavich, P. M., et al. 2004, *ApJ*, 613, 1120
- Gerardy, C., et al. 2004, *ApJ*, 607, 391
- Hamuy, M., et al. 2002, *AJ*, 124, 417
- Hatano, K., Branch, D., Fisher, A., Baron, E., & Filippenko, A. V. 1999b, *ApJ*, 525, 881
- Hatano, K., Branch, D., Fisher, A., Millard, J., & Baron, E. 1999a, *ApJS*, 121, 233
- Hatano, K., Branch, D., Qiu, Y. L., Baron, E., Thielemann, F.-K., & Fisher, A. 2002, *New Astr.*, 7, 441
- Hernandez, M., et al. 2000, *MNRAS*, 319, 223

- Hillebrandt, W., Sim, S. A., & Röpke, F. K. 2007, *A&A*, 465, L17
- Howell, D. A., Höflich, P., Wang, L., & Wheeler, J. C. 2001, *ApJ*, 556, 302
- Howell, D. A., et al. 2006, *Nature*, 443, 308
- Jeffery, D. J. & Branch, D. 1990, in *Supernovae*, eds. J. C. Wheeler, T. Piran, & S. Weinberg (Singapore: World Scientific), 149
- Jeffery, D. J., Branch, D., & Baron, E. 2007a, *ApJ*, submitted
- Jeffery, D. J., Ketchum, W., Branch, D., Baron, E., Elmhamdi, A., & Danziger, I. J. 2007b, *ApJS*, in press
- Jeffery, D. J., Leibundgut, B., Kirshner, R. P., Benetti, S., Branch, D., & Sonneborn, G. 1992, *ApJ*, 397, 304
- Jha, S., et al. 2006, *AJ*, 132, 189
- Kasen, D., & Woosley, S. E. 2007, *ApJ*, 656, 661
- Kasen, D., et al. 2003, *ApJ*, 593, 788
- Kotak, R., et al. 2006, *A&A*, 436, 1021
- Krisciunas, K., et al. 2006, *AJ*, 133, 58
- Leibundgut, B., Kirshner, R. P., Filippenko, A. V., Shields, J. S, Foltz, C. B., Phillips, M. M., & Sonneborn, S. 1991, *ApJ*, 371, L23
- Li, W., et al. 1999, *AJ*, 117, 2709
- Li, W., et al. 2001, *PASP*, 113, 1178
- Li, W., et al. 2003, *PASP*, 115, 453
- Marion, G. H., Höflich, P., Wheeler, J. C., Robinson, E. L., Gerardy, C. L., & Vacca, W. D. 2006, *ApJ*, 645, 1392
- Mattila, S., et al. 2005, *A&A*, 443, 649
- Mazzali, P. A. 2001, *MNRAS*, 321, 341
- Mazzali, P. A., Benetti, S., & Hillebrandt, W. 2007, *Science*, 315, 825
- Mazzali, P. A., Danziger, I. J., & Turatto, M. 1995, *A&A* 297, 509
- Mazzali, P. A., Lucy, L. B., Danziger, I. J., Gouiffes, C., Cappellaro, E., & Turatto, M. 1993, *A&A* 269, 423
- Mazzali, P. A., et al. 2005a, *MNRAS*, 357, 200
- Mazzali, P. A., et al. 2005b, *ApJ*, 623, L37
- McCall, M. L., Reid, N., Bessell, M. S., & Wickramasinghe, D. 1984, *MNRAS*, 210, 839

- Meikle, W. P. S., et al. 1996, MNRAS, 281, 263
- Nugent, P., Phillips, M. M., Baron, E., Branch, D., & Hauschildt, P. H. 1995, ApJ, 455, L147
- Parrent, J., et al. 2007, PASP, 119, 135
- Pastorello et al. 2007, MNRAS, 377, 1531
- Phillips, M. M., Lira, P., Suntzeff, N. B., Schommer, R. A., Hamuy, M., & Maza, J. 1999, AJ, 118, 1766
- Phillips, M. M., Wells, L. A., Suntzeff, N. B., Hamuy, M., Leibundgut, B., Kirshner, R. P., & Foltz, C. B. 1992, AJ, 103, 1632
- Phillips, M. M., et al. 2007, PASP, 119, 360
- Quimby, R., et al. 2006, ApJ, 636, 400
- Ruiz-Lapuente, P., Cappellaro, E., Turatto, M., Gouiffes, C., Danziger, I. J., Della Valle, M., & Lucy, L. B. 1992, ApJ, 387, L33
- Stanishev, V., et al. 2007, A&A, in press
- Stehle, M., Mazzali, P. A., Benetti, S., & Hillebrandt, W. 2005, MNRAS, 360, 1231
- Tanaka, M., Mazzali, P. A., Maeda, K., & Nomoto, K. 2006, ApJ, 645, 470
- Thomas, R. C., Branch, D., Baron, E., Nomoto, K., Li, W., & Filippenko, A. V. 2004, ApJ, 601, 1019
- Thomas, R. C., et al. 2007, ApJ, 654, L53
- Valentini, G., et al. 2003, 595, 779
- Wang, L., et al. 2003, ApJ, 591, 1110
- Wegner, G., & McMahan, R. K. 1987, AJ, 92, 287
- Wells, L. A., et al. 1994, AJ, 108, 2233

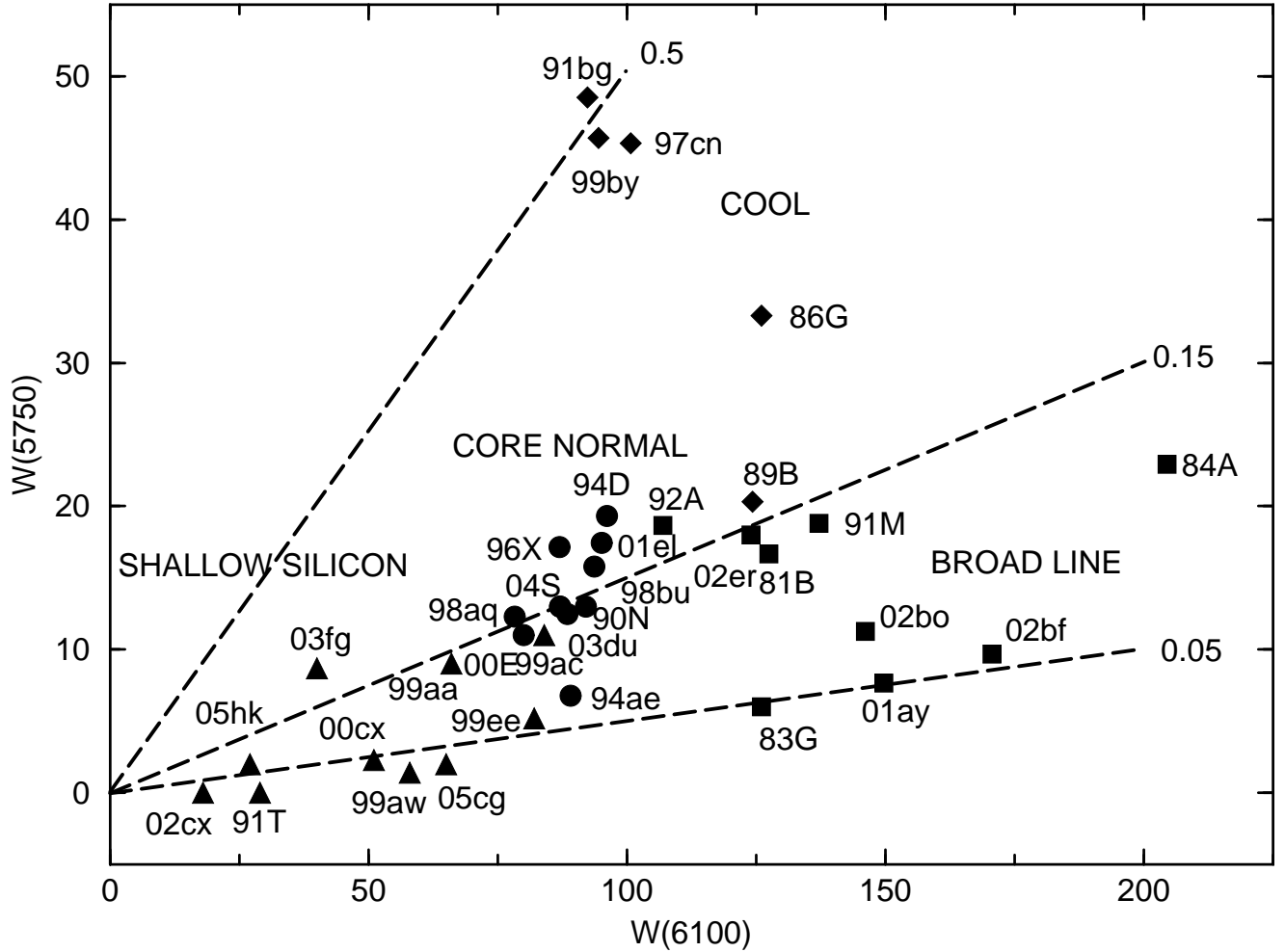


Fig. 1.— An update of Figure 1 of Paper II: $W(5750)$ is plotted against $W(6100)$ for spectra obtained within three days of maximum light. Core-normal SNe Ia are shown as *circles*, broad-line SNe Ia as *squares*, cool SNe Ia as *diamonds*, and shallow-silicon SNe Ia as *triangles*. The labels of the *dashed lines* refer to the $W(5750)/W(6100)$ ratio.

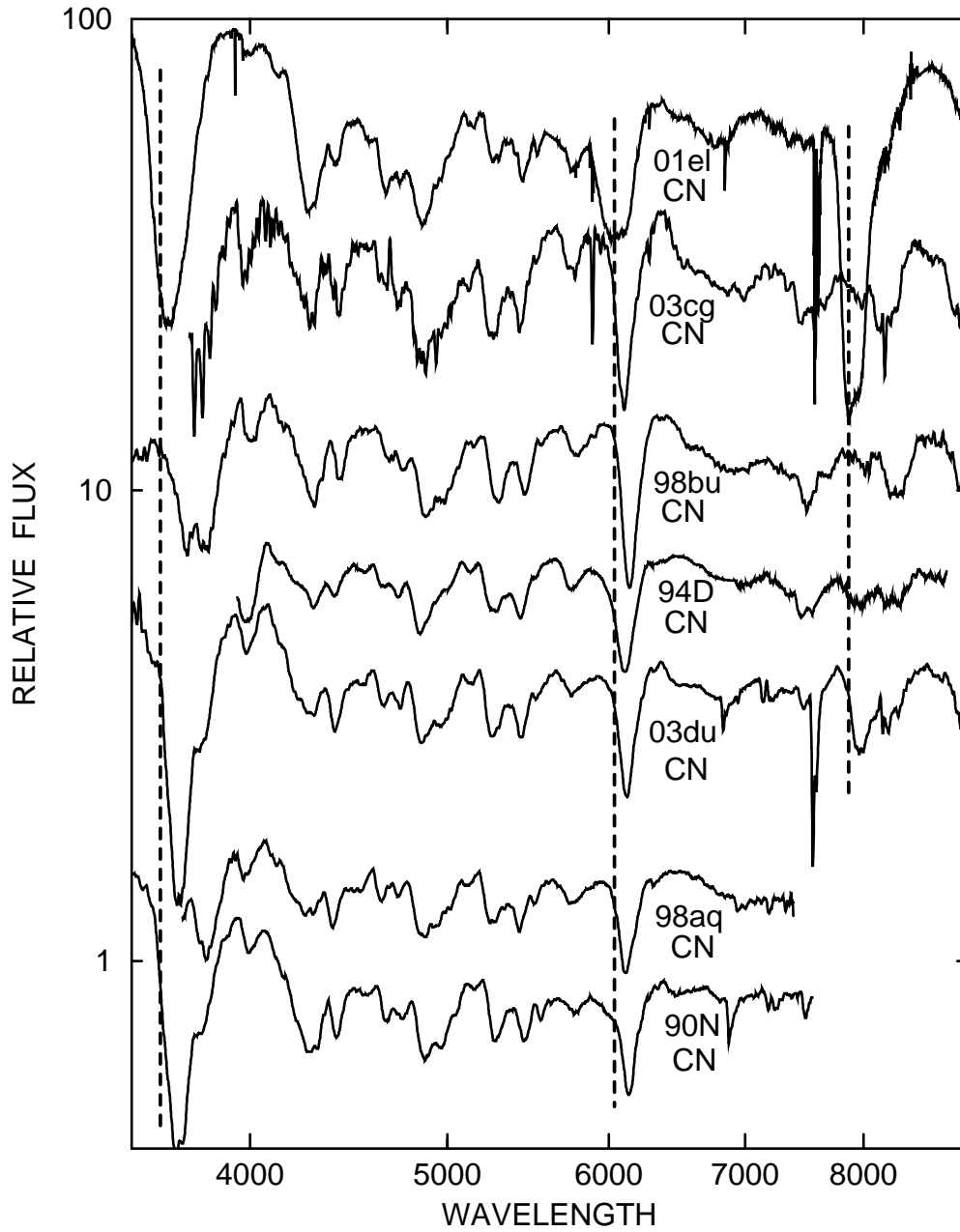


Fig. 2.— Spectra of seven core-normals of the one-week premax sample. The spectra have been flattened as described in the text. Vertical displacements are arbitrary and narrow absorptions near 7600 Å and 6900 Å are telluric. Vertical *dashed lines* refer to Ca II λ 3945 and λ 8579 blueshifted by 25,000 km s⁻¹ and Si II λ 6355 blueshifted by 15,000 km s⁻¹.

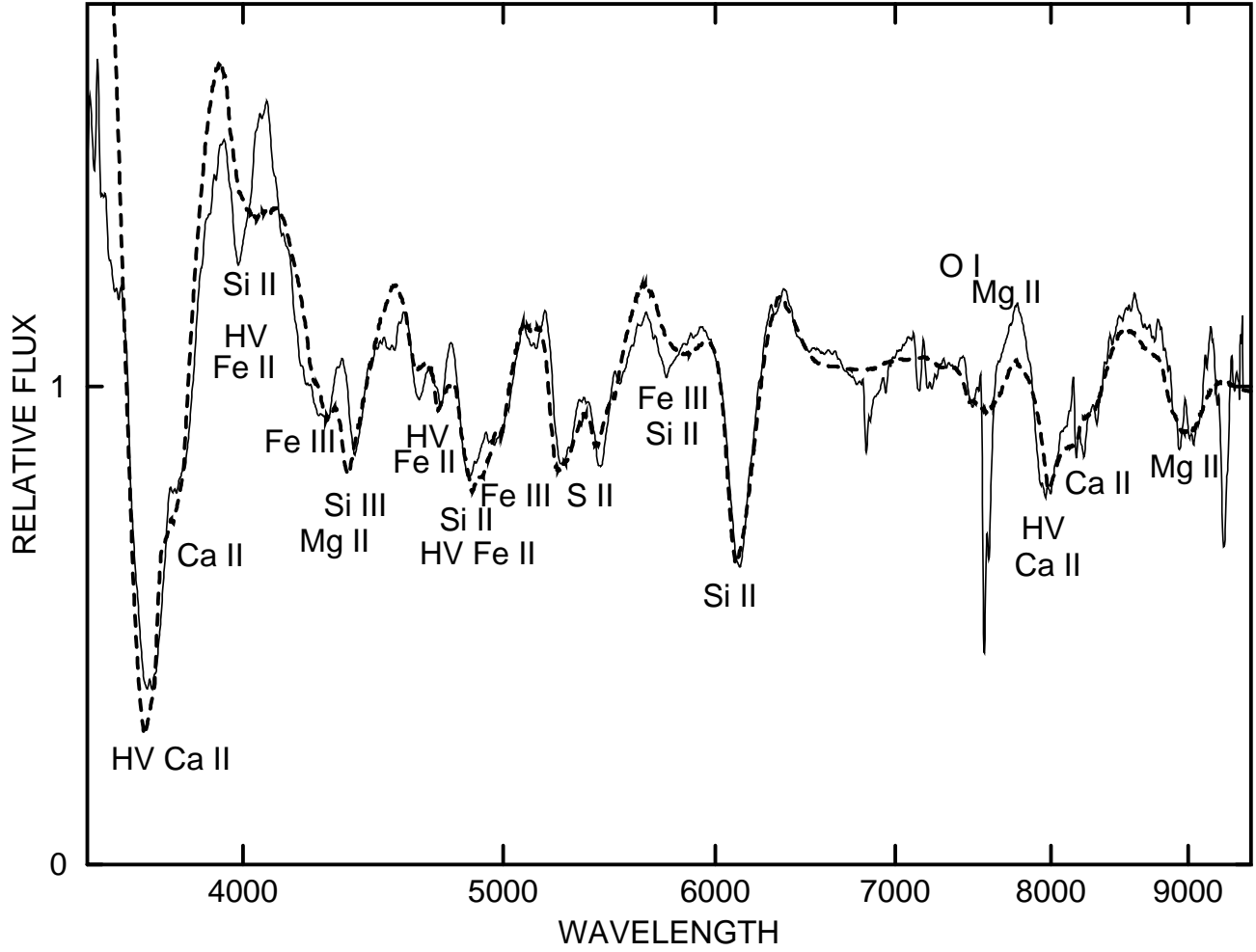


Fig. 3.— The day -7 spectrum of the core-normal SN 2003du (*solid line*), from Anupama et al. (2005), is compared with a synthetic spectrum (*dashed line*).

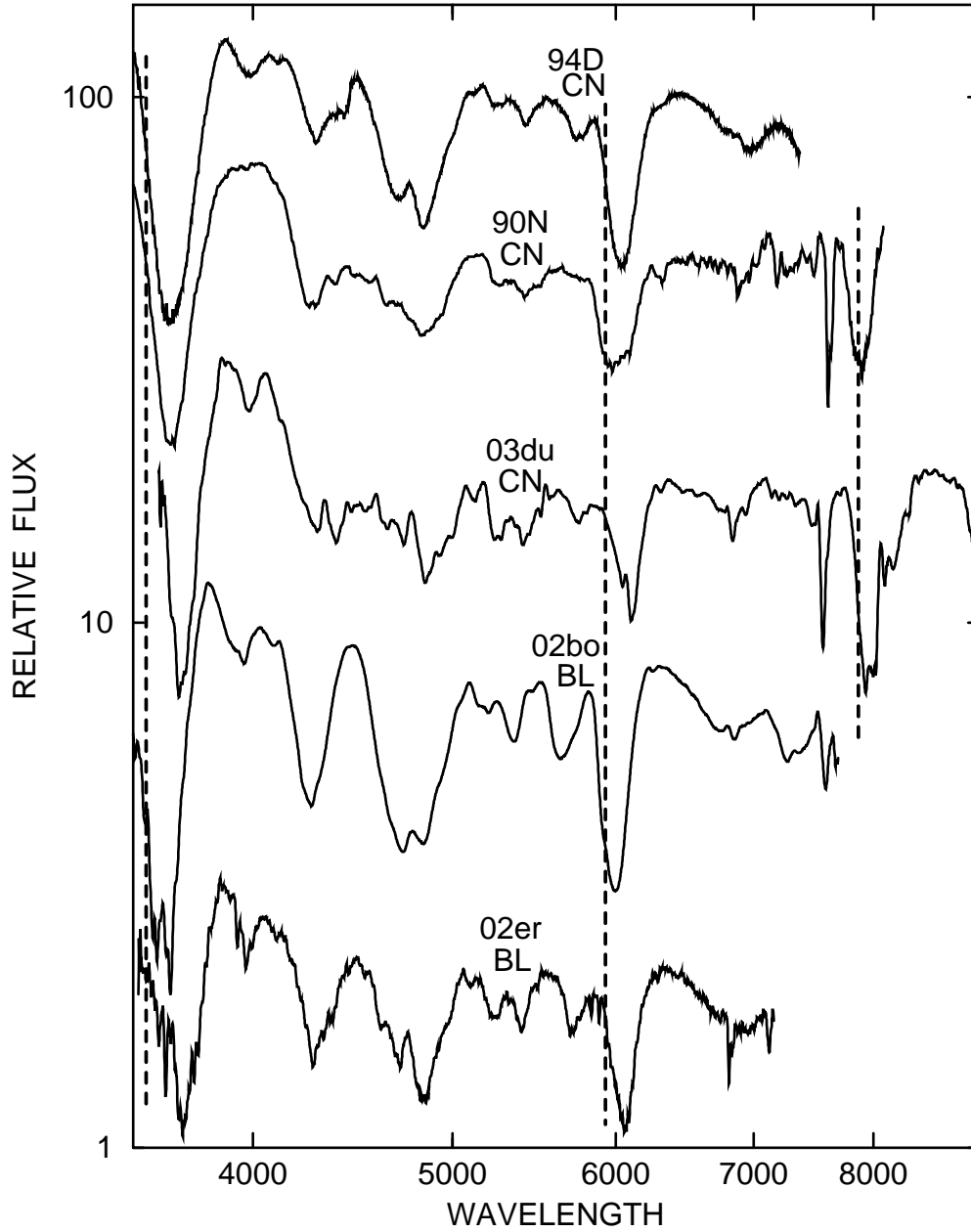


Fig. 4.— Spectra of three core-normals and two broad-lines of the early sample. Vertical *dashed lines* refer to Ca II $\lambda 3945$ blueshifted by $30,000 \text{ km s}^{-1}$, Si II $\lambda 6355$ blueshifted by $20,000 \text{ km s}^{-1}$, and Ca II $\lambda 8579$ by $25,000 \text{ km s}^{-1}$.

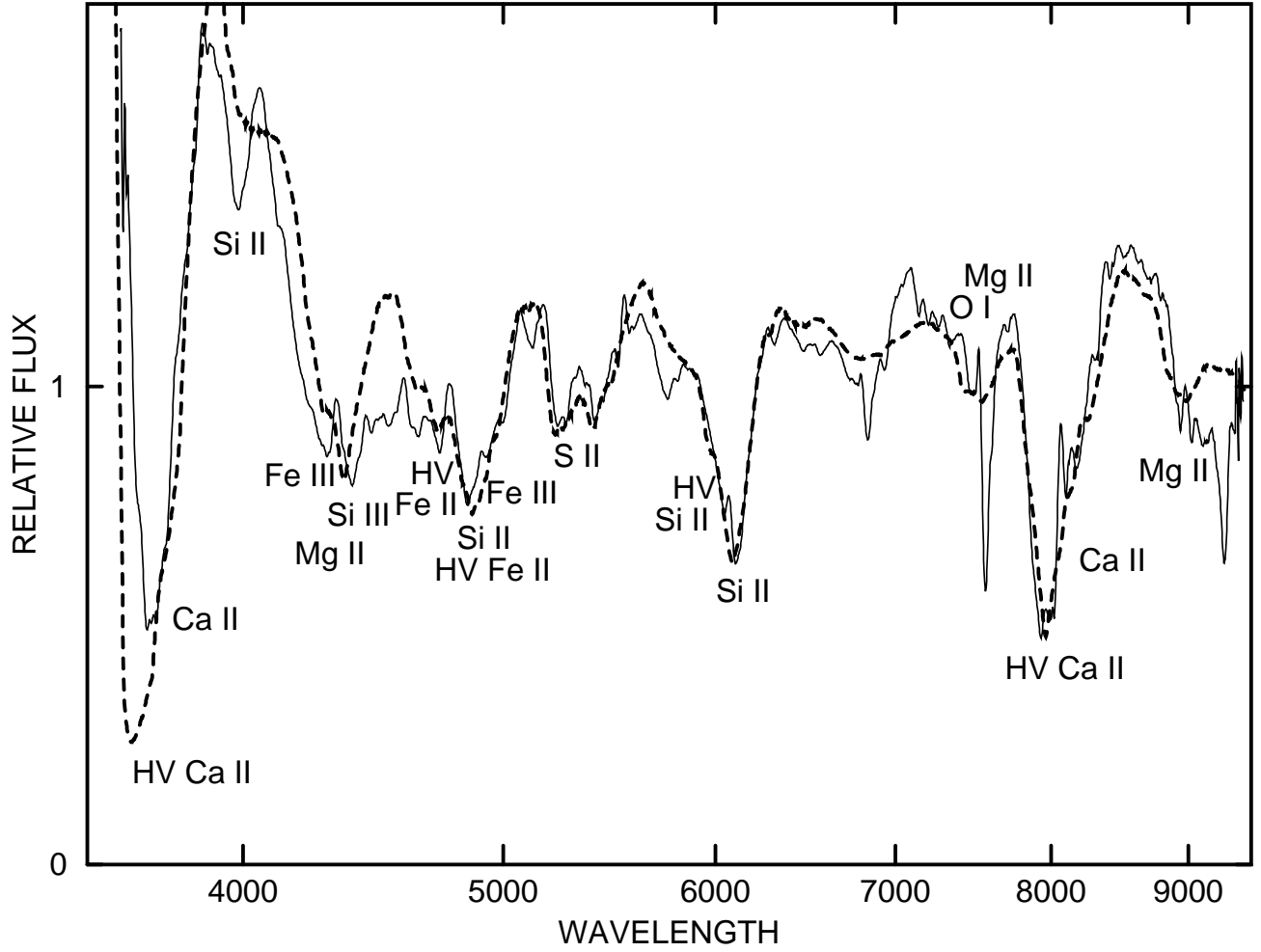


Fig. 5.— The day -11 of the core-normal SN 2003du (*solid line*), from Stanishev et al. (2007), is compared with a synthetic spectrum (*dashed line*).

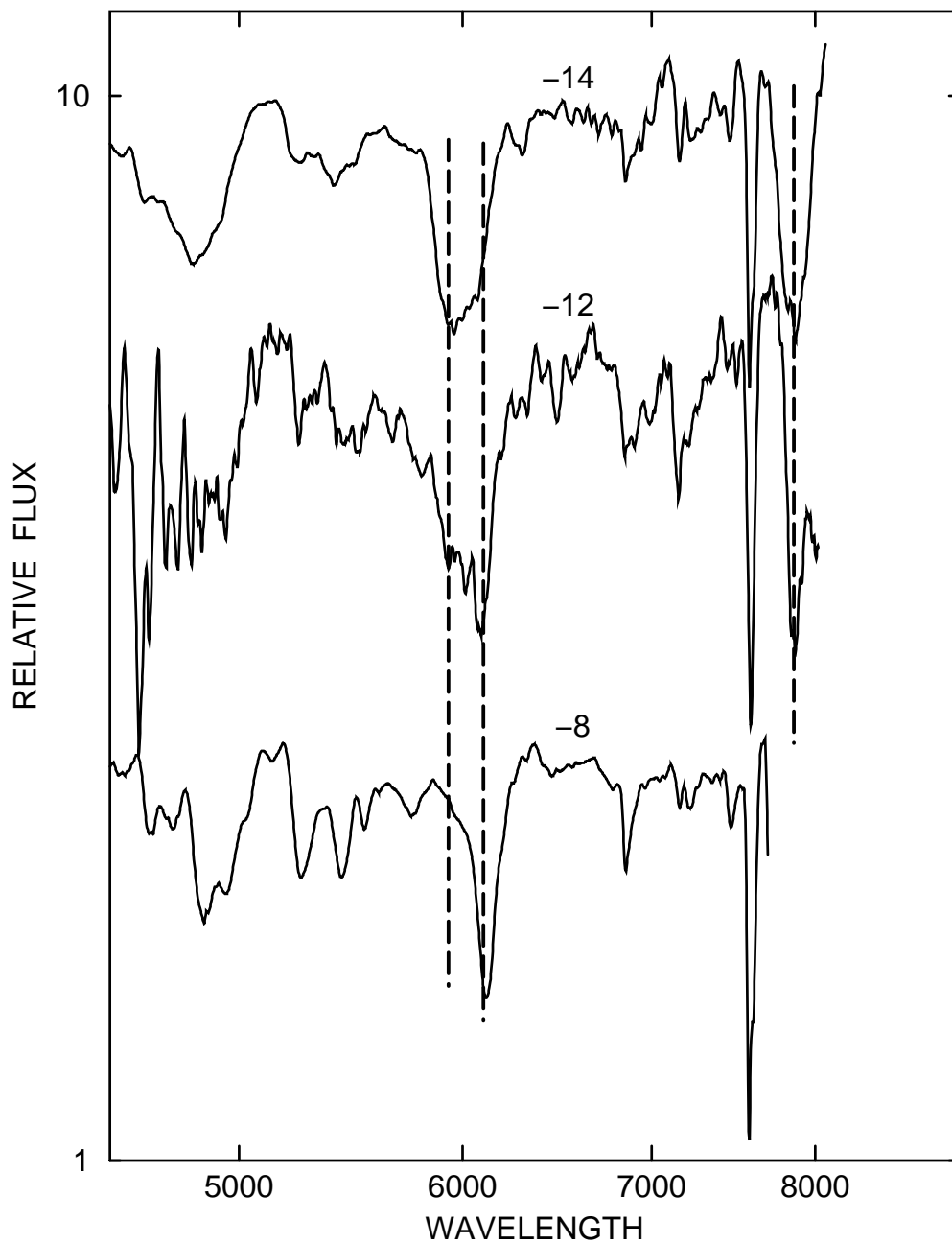


Fig. 6.— Three spectra of SN 1990N are compared: days -14 and -8 , from Leibundgut et al. (1991), and a previously unpublished spectrum obtained on day -12 by S. Benetti and M. Turatto. Vertical *dashed lines* refer to Si II $\lambda 6355$ blueshifted by $20,000$ and $12,000$ km s^{-1} and Ca II $\lambda 8579$ blueshifted by $25,000$ km s^{-1} . The 6100 \AA absorption in the day -12 spectrum appears to be a marginally resolved two-component (PV + HV) feature.

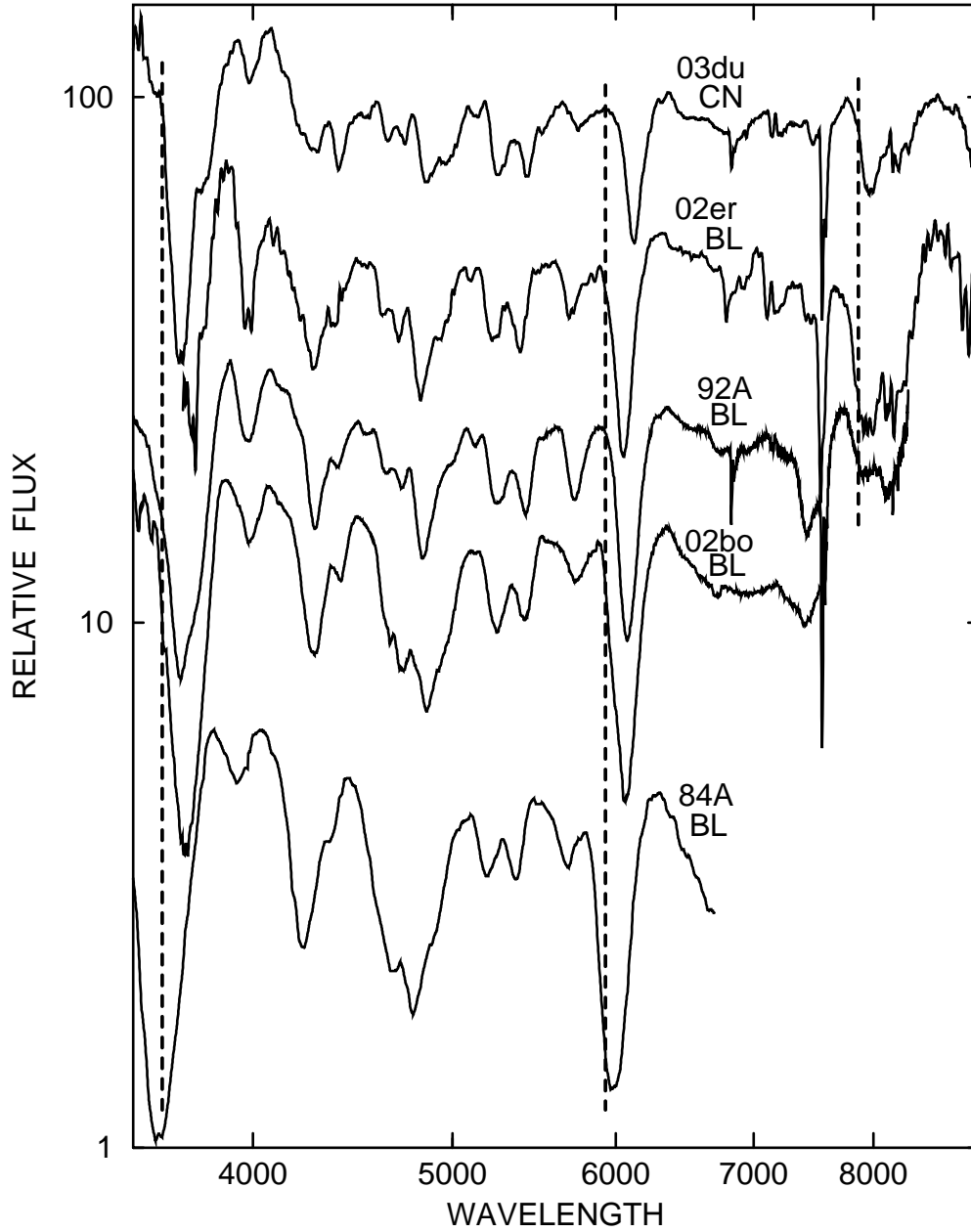


Fig. 7.— Spectra of one core-normal and four broad-line SN Ia of the one-week premax sample. Vertical *dashed lines* refer to Ca II $\lambda 3945$ and $\lambda 8579$ blueshifted by $25,000 \text{ km s}^{-1}$ and Si II $\lambda 6355$ blueshifted by $20,000 \text{ km s}^{-1}$.

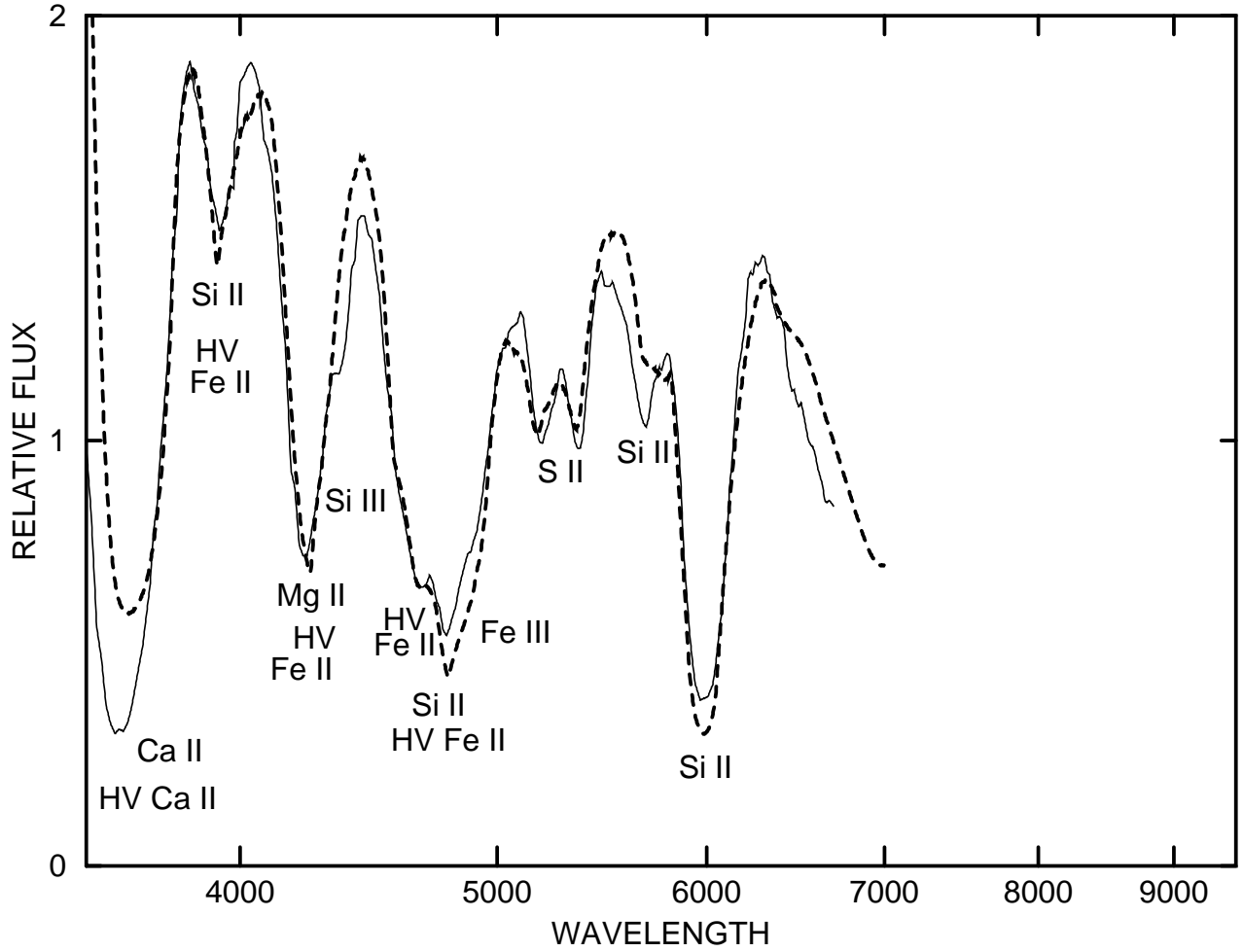


Fig. 8.— The day -7 spectrum of the extreme broad-line SN 1984A (*solid line*), from Wegner & McMahan (1987), is compared with a synthetic spectrum (*dashed line*).

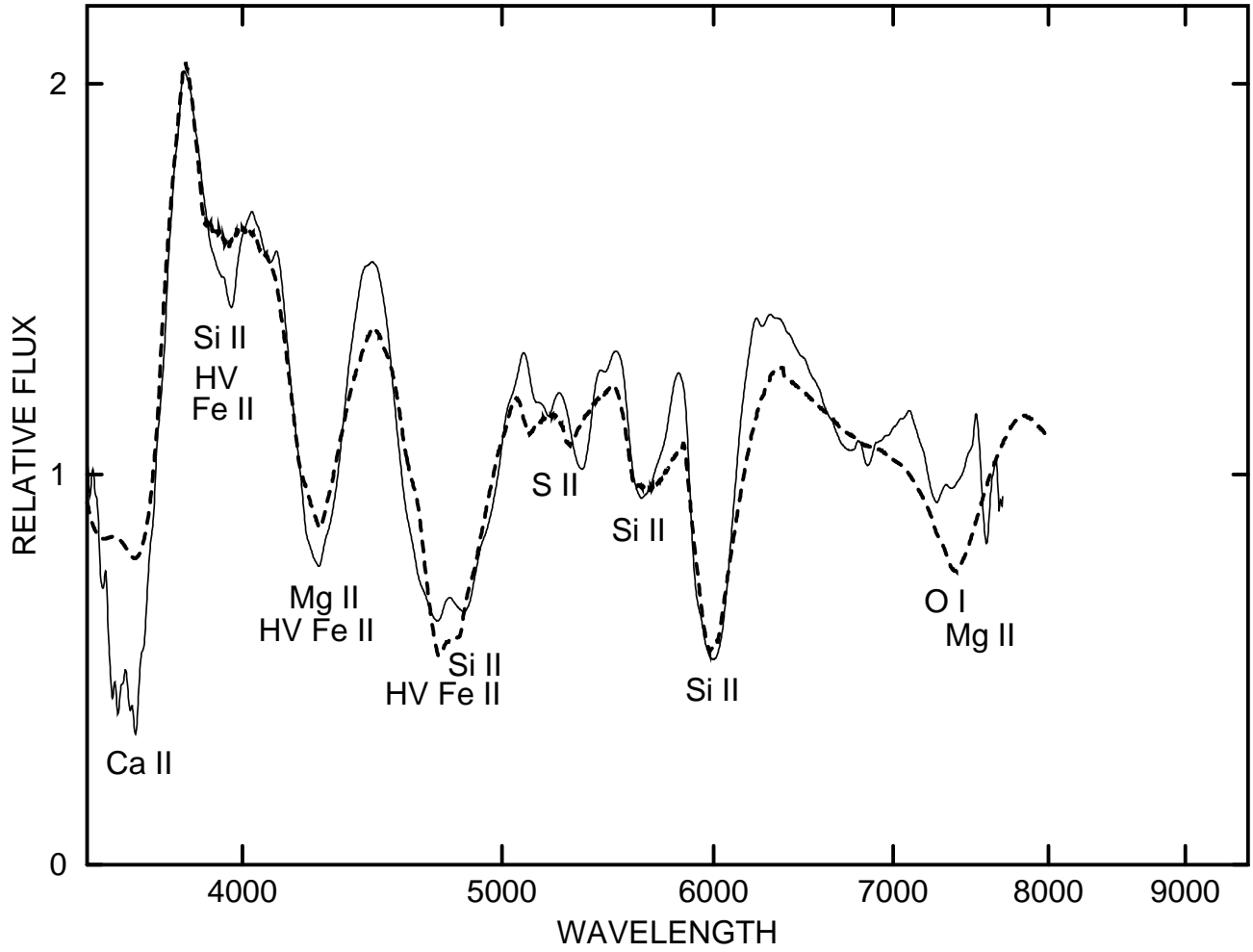


Fig. 9.— The day -14 spectrum of the broad-line SN 2002bo (*solid line*), from Benetti et al. (2004), is compared with a synthetic spectrum (*dashed line*).

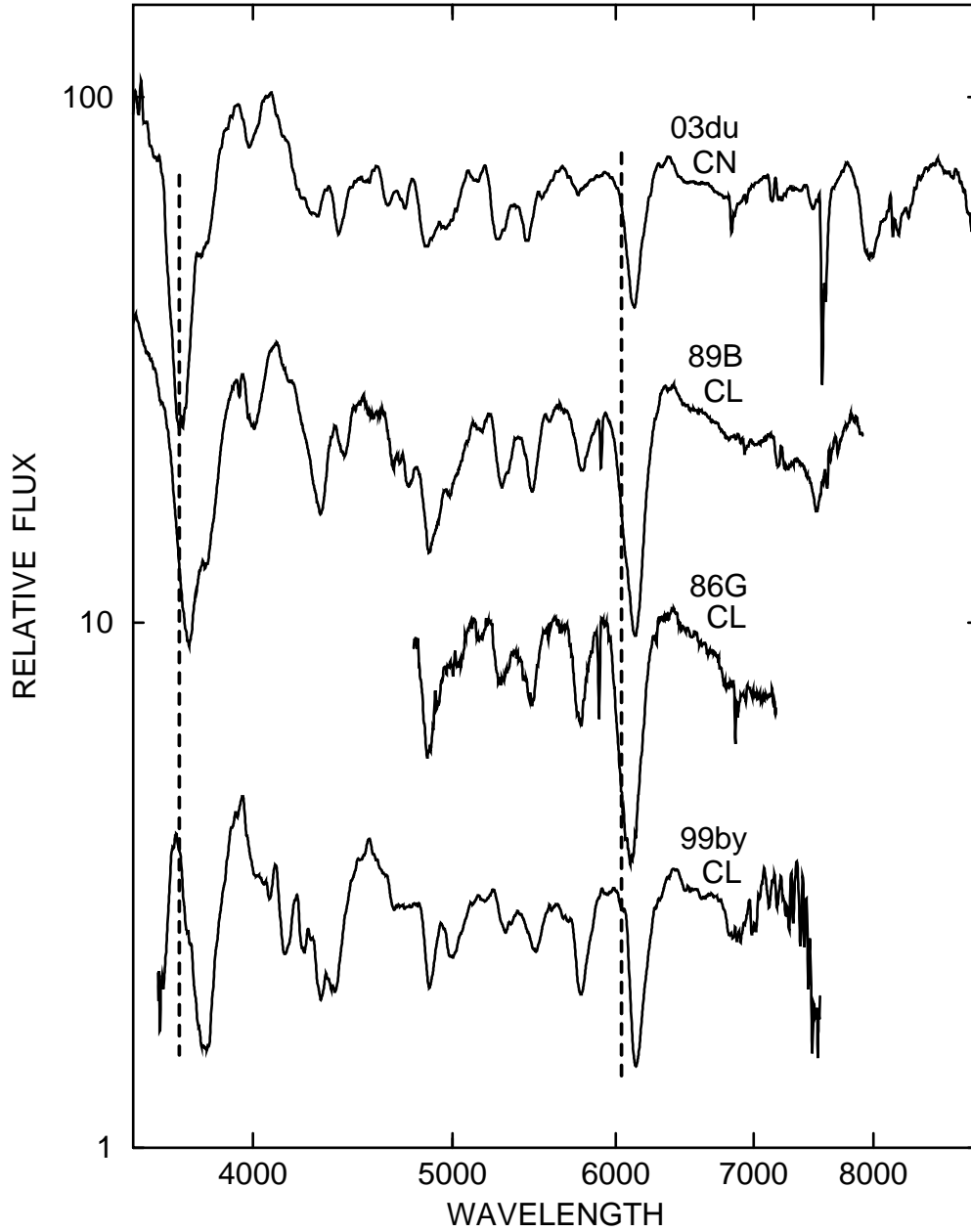


Fig. 10.— Spectra of one core-normal and three cools of the one-week premax sample. Vertical dashed lines refer to Ca II λ 3945 blueshifted by 20,000 km s⁻¹ and Si II λ 6355 blueshifted by 15,000 km s⁻¹.

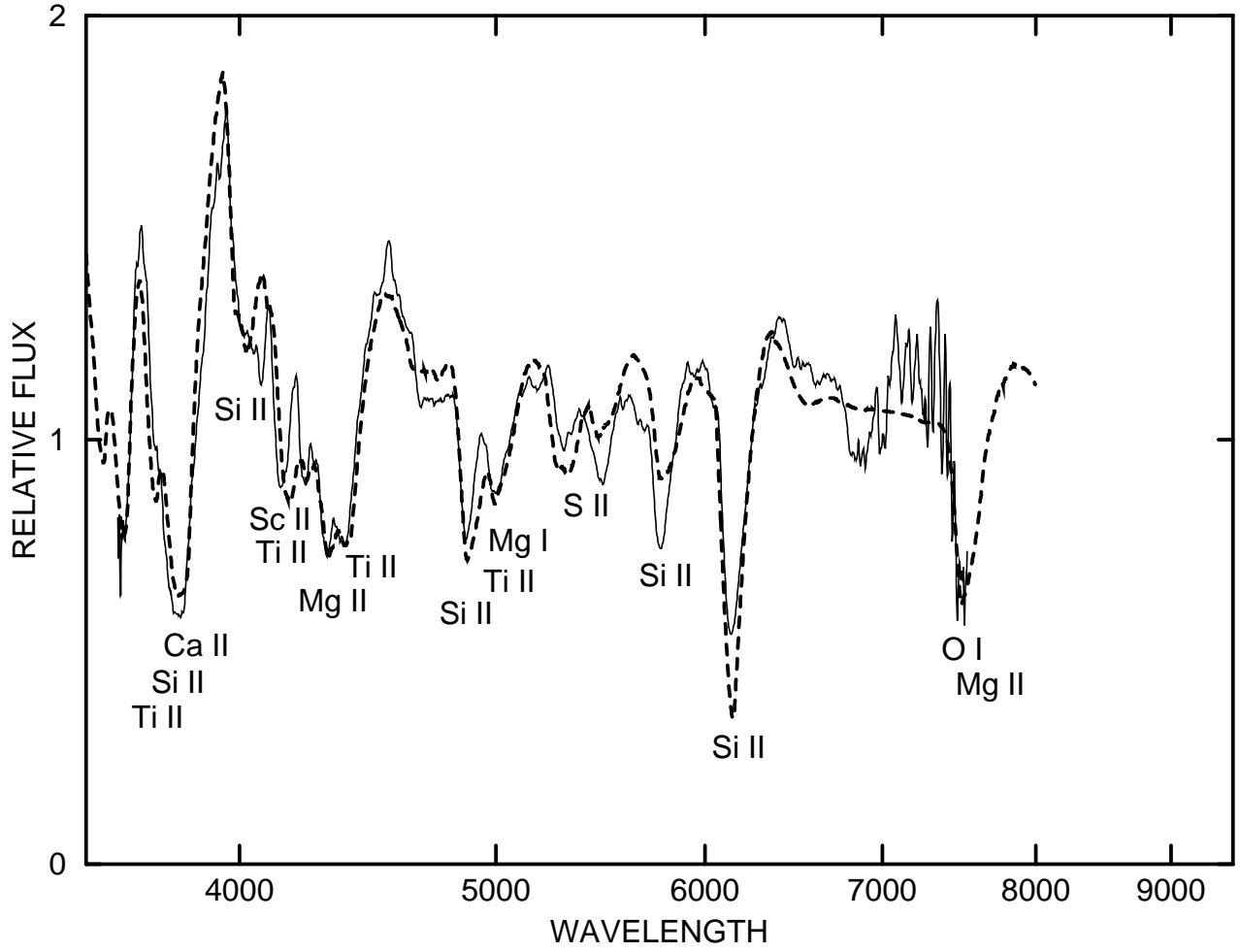


Fig. 11.— The day -5 spectrum of the cool SN 1999by (*solid line*), from Garnavich et al. (2004), is compared with a synthetic spectrum (*dashed line*).

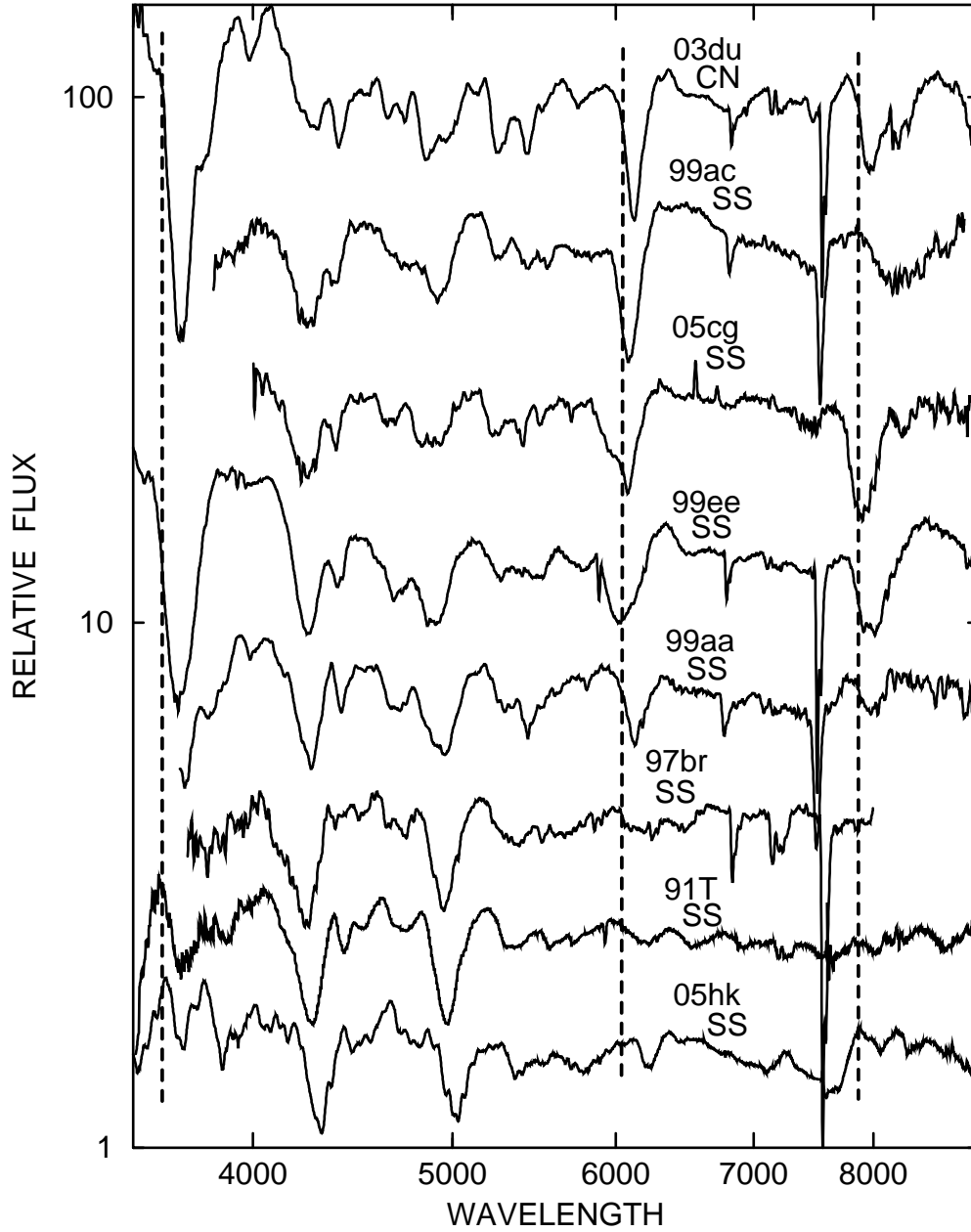


Fig. 12.— Spectra of one core-normal and seven shallow-silicons of the one-week premax sample. Vertical *dashed lines* refer to Ca II $\lambda 3945$ and $\lambda 8579$ blueshifted by $25,000 \text{ km s}^{-1}$ and Si II $\lambda 6355$ blueshifted by $15,000 \text{ km s}^{-1}$.

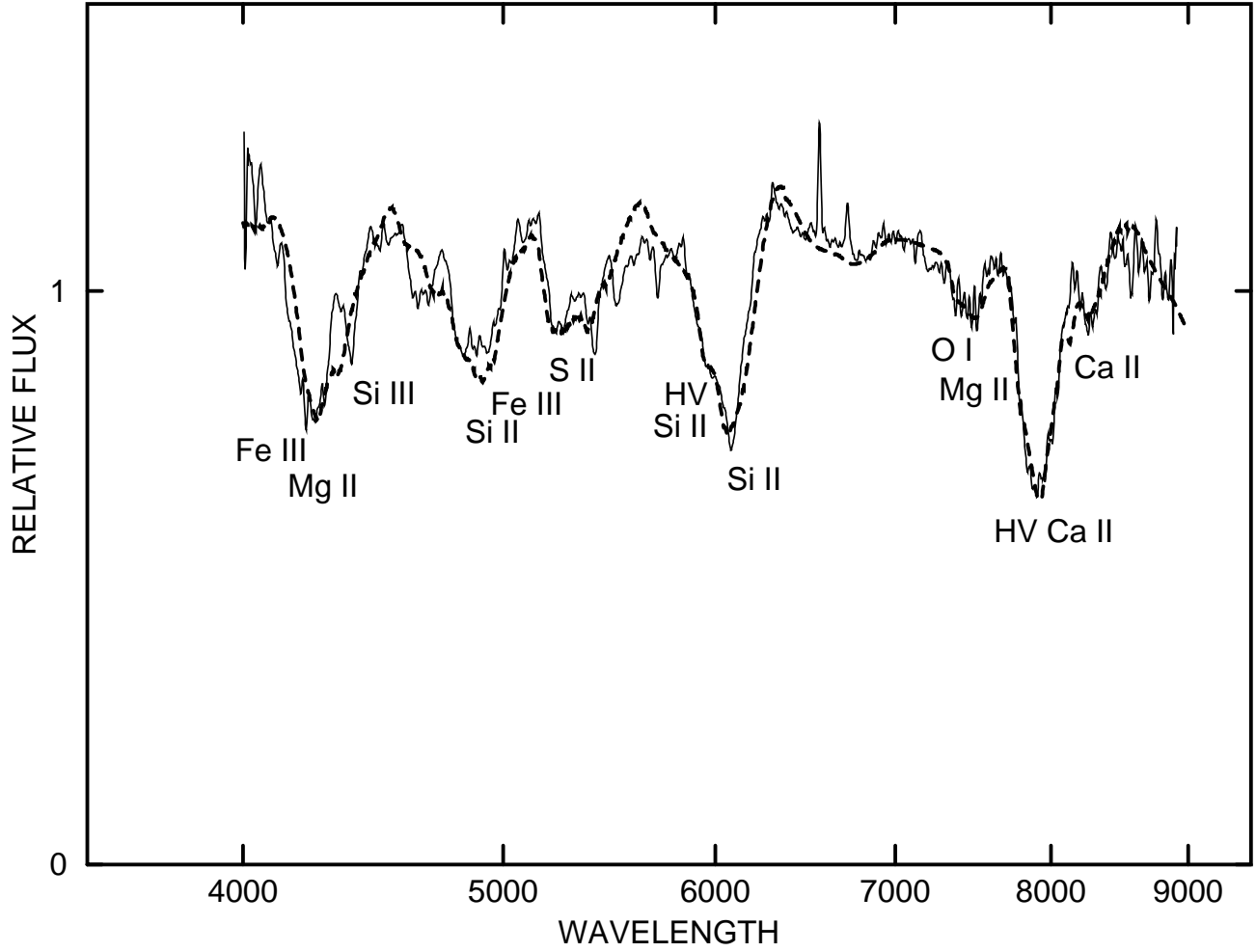


Fig. 13.— The day -9 spectrum of the shallow-silicon SN 2005cg (*solid line*), from Quimby et al. (2006), is compared with a synthetic spectrum (*dashed line*).

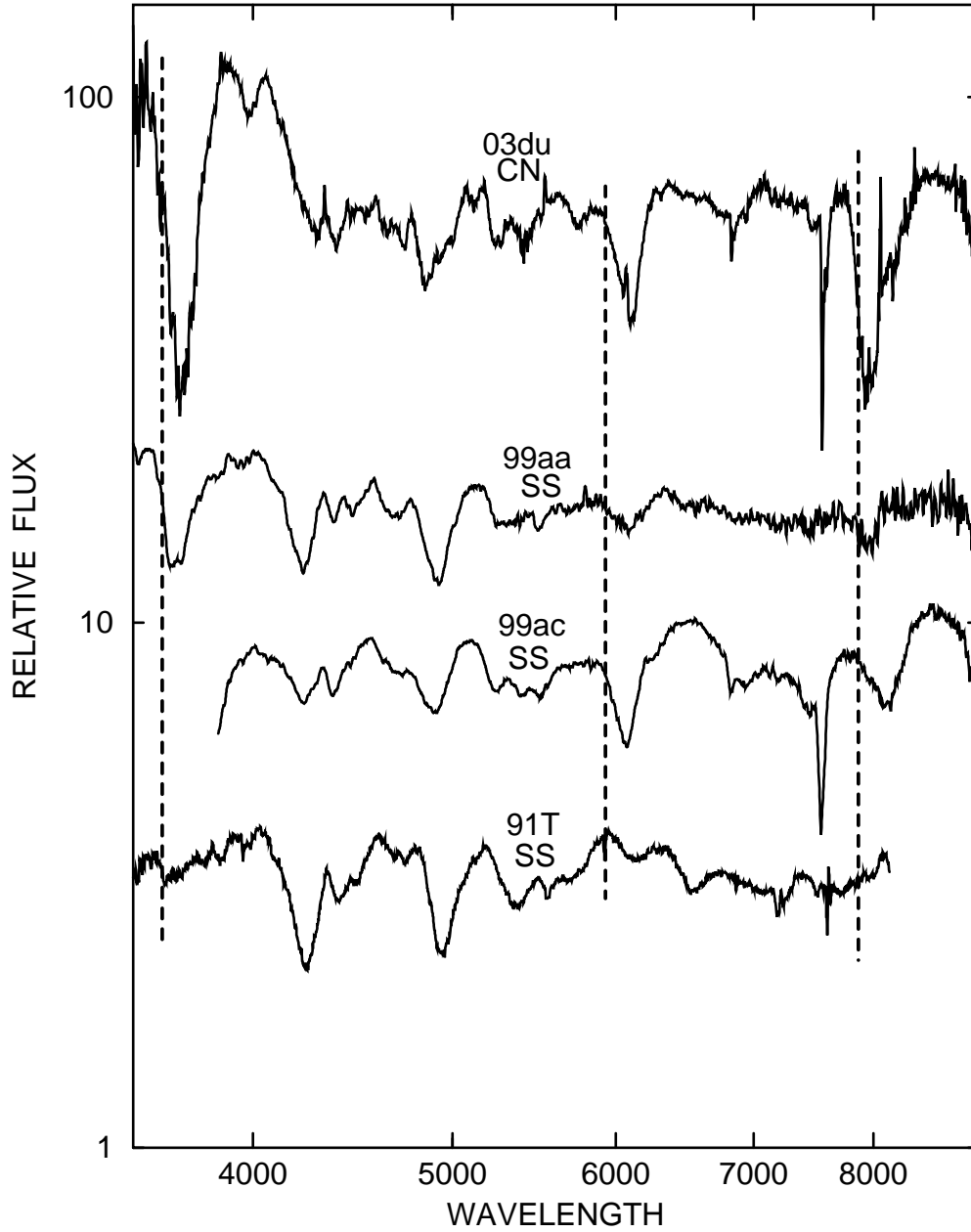


Fig. 14.— Spectra of one core-normal and three shallow-silicons of the early sample. Vertical *dashed lines* refer to Ca II $\lambda 3945$ and $\lambda 8579$ blueshifted by $25,000 \text{ km s}^{-1}$ and Si II $\lambda 6355$ blueshifted by $20,000 \text{ km s}^{-1}$.

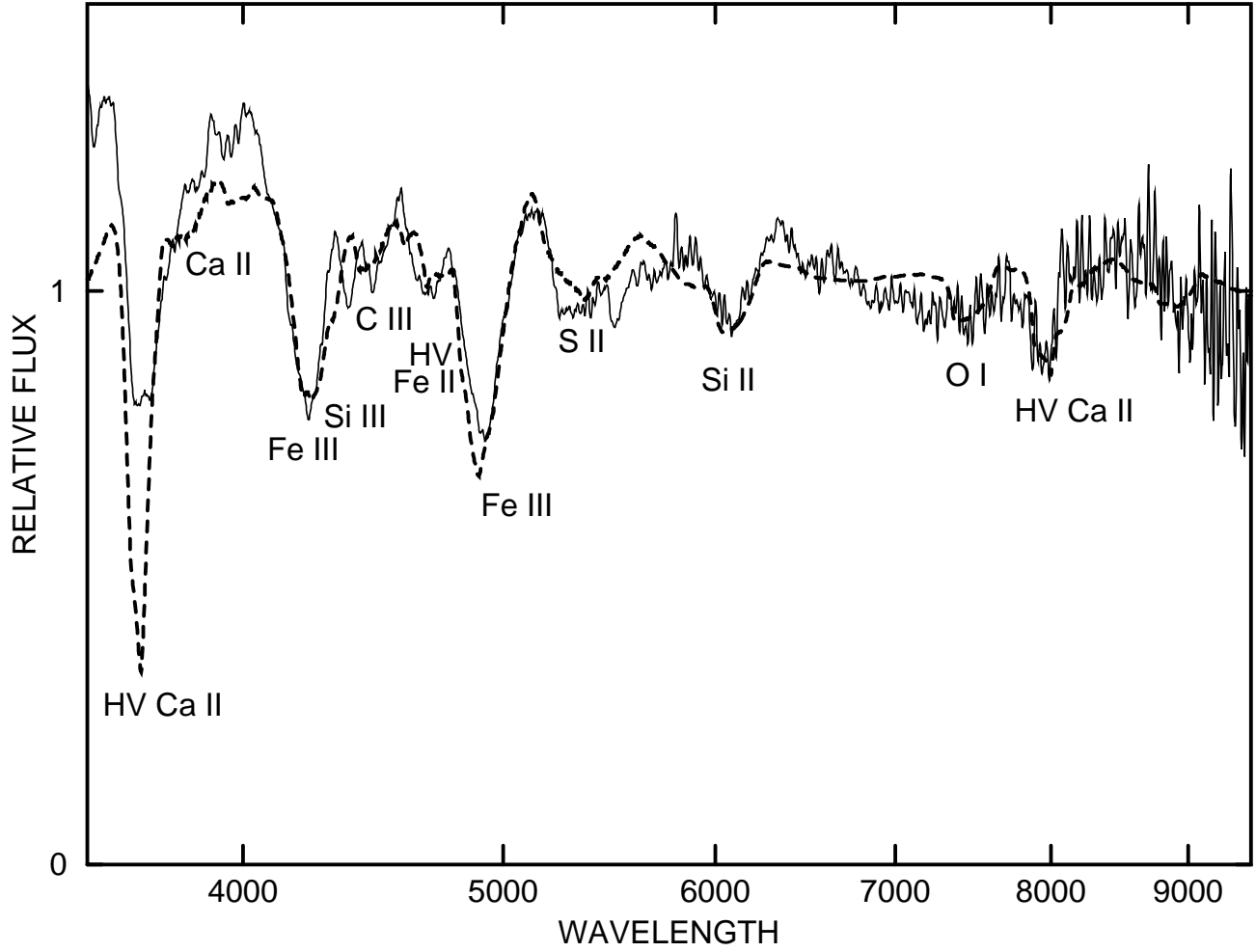


Fig. 15.— The day -12 spectrum of the shallow-silicon SN 1999aa (*solid line*), from Garavini et al. (2004), is compared with a synthetic spectrum (*dashed line*).

Table 1. The SN Ia Sample

SN	Epochs (days)	Galaxy	References
1984A BL	–7	NGC 4419	Wegner & McMahan (1987)
1986G CL	–6	NGC 5128	Cristiani et al. (1992)
1989B CL	–7	NGC 3627	Wells et al. (1994)
1990N CN	–8, –14	NGC 4639	Leibundgut et al. (1991)
1991T SS	–7, –11	NGC 4527	Phillips et al. (1992)
1992A BL	–6	NGC 1380	P. Challis, unpublished
1994D CN	–8, –12	NGC 4526	Meikle et al. (1996)
1997br SS	–7	ESO 576-G40	Li et al. (1999)
1998aq CN	–8	NGC 3982	Branch et al. (2003)
1998bu CN	–6	NGC 3368	Hernandez et al. (2000)
1999aa SS	–7, –12	NGC 4469	Garavini et al. (2004)
1999ac SS	–9, –15	NGC 2848	Garavini et al. (2005)
1999by CL	–5	NGC 2841	Garnavich et al. (2004)
1999ee SS	–7	IC 5179	Hamuy et al. (2002)
2001el CN	–8	NGC 1448	Mattila et al. (2005)
2002bo BL	–6, –14	NGC 3190	Benetti et al. (2004)
2002er BL	–7, –11	UGC 10743	Kotak et al. (2006)
2003cg CN	–7	NGC 3169	Elias-Rosa et al. (2006)
2003du CN	–7, –11	NGC 1921	Anupama et al. (2005), Stanishev et al. (2007)
2005cg SS	–9	NGC 9290	Quimby et al. (2006)
2005hk SS	–5	UGC 272	Chornock et al. (2006)

Table 2. Fitting Parameters for Core–Normal SNe Ia of the One–Week Premax Sample

Parameter	SN 1990N	SN 1994D	SN 1998aq	SN 1998bu	SN 2001el	SN 2003cg	SN 2003du
v_{phot} (km s ⁻¹)	12,000	13,000	13,000	11,000	15,000	13,000	13,000
v_e (km s ⁻¹)	1000	1000	1000	1000	2000	1000	1000
$\tau(\text{C II})$...	0.8	0.4/14
$\tau(\text{O I})$...	0.5/14	...	0.6/12	...	0.8	0.3
$\tau(\text{Mg II})$	1.2	0.5	0.4	1.5	0.5	0.7	0.5
$\tau(\text{Si II})$	4	5	5	8	2	8	5
$\tau(\text{HV Si II})$	0.5/20	8	5
$\tau(\text{Si III})$	1.1	0.6	1.8	1.8	0.2	1.7	2.2
$\tau(\text{S II})$	1.7	1.5	1.5	2	0.4	3	1.8
$\tau(\text{Ca II})$	5(2)	10	4	25	...	25	6(2)
$\tau(\text{HV Ca II})$	1.8(4)/20	2.5(3)/23	...	1.6(2)/20	20(8)/23[34]	5/22	5(3)/21
$\tau(\text{HV Fe II})$	0.2(3)/17	0.25(2)/19	0.2(2)/19	0.2(2)/17	1/20	0.4/19	0.4/19
$\tau(\text{Fe III})$	1.2	0.5	0.7	1.5	...	1.5	0.8

^aFor each ion the optical depth, τ , is the optical depth at the photosphere or detachment velocity of the ion’s reference line (ordinarily the ion’s strongest line in the optical spectrum). When a value of v_e other than the default value in row 2 is used, the value (in units of 1000 km s⁻¹) is given in parentheses. Minimum and maximum velocities (in units of 1000 km s⁻¹) are preceded by a forward slash. Maximum velocities are in square brackets.

Table 3. Fitting Parameters for Three Core–Normal and Two Broad–line SNe Ia of the Early Sample

Parameter	SN 1990N	SN 1994D	SN 2003du	SN 2002bo	SN 2002er
v_{phot} (km s ⁻¹)	14,000	14,000	14,000	20,000	15,000
v_e (km s ⁻¹)	2000	2000	1000	2000	2000
$\tau(\text{C II})$	0.5	0.6	0.6
$\tau(\text{O I})$...	0.5	0.3/15	0.2(3)/21	...
$\tau(\text{Mg II})$	0.6	1	1
$\tau(\text{Si II})$	1.6	8	8	30[25]	6[20]
$\tau(\text{HV Si II})$	0.7(3)/20	...	0.5(2)/20
$\tau(\text{Si III})$	0.3	0.7	2.5	0.6	0.2
$\tau(\text{S II})$	0.5	0.6	1.8	1[22]	1.5[16]
$\tau(\text{Ca II})$...	200	12(2)	20(10)	10
$\tau(\text{HV Ca II})$	8(6)/24[30]	200(6)/23	12(5)/22	...	100(6)/23
$\tau(\text{HV Fe II})$	0.3(3)/20	1.2(3)/20	0.3(3)/19	1(3)/22	0.7(3)/20
$\tau(\text{Fe III})$	0.5	...	0.8

^aFor column descriptions see the note to Table 2.

Table 4. Fitting Parameters for Broad-Line SNe Ia of the One-Week Premax Sample

Parameter	SN 1984A	SN 1992A	SN 2002bo	SN 2002er
v_{phot} (km s ⁻¹)	16,000	14,000	14,000	16,000
v_e (km s ⁻¹)	2000	1000	2000	1000
$\tau(\text{O I})$...	1.5/16	0.15(3)/15	0.1
$\tau(\text{Mg II})$	3	1.2(2)	0.8	1.7(2)
$\tau(\text{Si II})$	10(4)/[27]	45	7	35
$\tau(\text{Si III})$	0.6	0.5	0.5	0.7
$\tau(\text{S II})$	2.3	2.5	1.7	3.5
$\tau(\text{Ca II})$	20(6)	50	120	150
$\tau(\text{HV Ca II})$	20(6)/21	2(20)/24[28]	5(3)/21	8(20)/24[29]
$\tau(\text{HV Fe II})$	1.7(3)/24	0.8/19	1(3)/19	1.5/20
$\tau(\text{Fe III})$	1.4	0.5	1	0.4

^aFor column descriptions see the note to Table 2.

Table 5. Fitting Parameters for Cool SNe Ia of the One-Week Premax Sample

	SN 1989B	SN 1986G	SN 1999by
v_{phot} (km s ⁻¹)	12,000	12,000	11,000
v_e (km s ⁻¹)	1000	1000	1000
$\tau(\text{O I})$	1/13	...	4
$\tau(\text{Mg I})$...	2.5	1.8
$\tau(\text{Mg II})$	1/13	...	2
$\tau(\text{Si II})$	20	40(2)/[19]	60/[14]
$\tau(\text{Si III})$	0.7
$\tau(\text{S II})$	2	2	1
$\tau(\text{Ca II})$	10(2)	...	40
$\tau(\text{HV Ca II})$	1(2)/20
$\tau(\text{Sc II})$	1.5
$\tau(\text{Ti II})$	1.5
$\tau(\text{HV Fe II})$	1/17
$\tau(\text{Fe III})$	1.5

^aFor column descriptions see the note to Table 2.

Table 6. Fitting Parameters for Shallow–Silicon SNe Ia of the One–Week Premax Sample

	SN 1999ee	SN 1991T	SN 1997br	SN2005hk	SN 1999aa	SN 1999ac	SN 2005cg
v_{phot} (km s ⁻¹)	13,000	10,000	12,000	5000	11,000	13,000	15,000
v_e (km s ⁻¹)	2000	1000	1000	2000	2000	2000	1000
$\tau(\text{C III})$...	0.3	...	0.3
$\tau(\text{O I})$	0.1	0.1	...	0.08/6	0.1/12	0.1/14	0.5/17
$\tau(\text{Mg II})$	0.4(3)	0.3	...	0.35/6	0.3(3)	0.4(3)/14	0.3(4)
$\tau(\text{Si II})$	0.9	0.2	0.2	0.2	0.6	1.8	4
$\tau(\text{HV Si II})$	0.4/19	0.45(2)/21
$\tau(\text{Si III})$	0.5	1.3	0.6	0.3	0.5	0.9	0.8
$\tau(\text{S II})$	0.4	0.25	0.5	0.4	1
$\tau(\text{Ca II})$	5	1	0.3	0.8	1.5(3)	4(3)	15
$\tau(\text{HV Ca II})$	4(9)/20[28]	0.6(3)/18	0.2(2)/18	...	1.3(9)/21[28]	1.5(6)/19[23]	5(20)/23[32]
$\tau(\text{Ti II})$	0.04
$\tau(\text{HV Fe II})$	0.5/22	0.2/21	0.3/19	...
$\tau(\text{Fe III})$	0.6	0.7(2)	0.8(2)	0.7	0.6	0.5	0.8
$\tau(\text{Co II})$	0.2
$\tau(\text{Ni II})$	0.1
$\tau(\text{Ni III})$...	0.1(2)	0.15	0.1

^aFor column descriptions see the note to Table 2.

Table 7. Fitting Parameters for Shallow-Silicon SNe Ia of the Early Sample

Parameter	SN 1999aa	SN 1999ac	SN 1991T
v_{phot} (km s ⁻¹)	16,000	17,000	14,000
v_e (km s ⁻¹)	1000	1000	1000
$\tau(\text{C II})$...	0.2/19	...
$\tau(\text{C III})$	0.7	...	0.5
$\tau(\text{O I})$	0.3/17	1	...
$\tau(\text{Si II})$	0.4/17	5	0.2
$\tau(\text{Si III})$	0.6	2.5	2
$\tau(\text{S II})$	0.5	1.2	0.5
$\tau(\text{Ca II})$	1	4(2)	1
$\tau(\text{HV Ca II})$	7/25	1.5(5)/20	...
$\tau(\text{HV Fe II})$	0.5/22
$\tau(\text{Fe III})$	2	1.5	2

^aFor column descriptions see the note to Table 2.